Sign effects of volatility and jumps in forex markets and a reappraisal of meteor showers and heat waves

Massimiliano Caporin[a] and Syed Jawad Hussain Shahzad[b]

Abstract

We evaluate the impact of signed realized semivariances and jumps, in the evolution of the volatility of exchange rates w.r.t leading currencies the US Dollar, the Euro, the UK Pound and the Japanese Yen using high frequency 5-minute interval data. We re-examine the meteor shower and heat wave hypotheses for four trading time zones i.e., New York, Tokyo and Sydney, London only and London and NY jointly. We find short-run asymmetries in the effect of positive and negative semivariances. Meteor showers exist when trading takes place between London and NY and from NY to Tokyo and Sydney and are profound for bad volatility. Jump variations influence the future volatility of the time zones where they originate.

Résumé

Nous évaluons l'impact des sauts et des semi-variances signés et réalisés, sur l'évolution de la volatilité des taux de change par rapport aux principales devises que sont le dollar américain, l'euro, la livre sterling et le yen japonais. Nous faisons cela en utilisant des données à haute fréquence d'intervalle de 5 minutes. Nous re- examinons les hypothèses de la pluie de météores et de la vague de chaleur pour quatre fuseaux horaires commerciaux, c'est-à-dire New York (NY), Tokyo et Sydney, Londres uniquement et Londres et NY conjointement. Nous trouvons des asymétries à court terme dans l'effet des semi-variances positives et négatives. Les pluies de météores existent lorsque les transactions ont lieu entre Londres et NY et de NY à Tokyo et Sydney, et sont profondes pour une mauvaise volatilité. Les variations de saut influencent la volatilité future des fuseaux horaires d'où elles proviennent.

Keywords: forex markets, good and bad volatility, signed jumps, meteor showers, heat waves

JEL codes F31, G15

[a]Department of Statistical Sciences, University of Padova, Italy. Email: massimiliano.caporin@unipd.it
[b]Montpellier Business School, France. Corresponding author. Email: j.syed@montpellier-bs.com

Acknowledgments: Special thanks to Angelo Ranaldo for guidance and invaluable advice. We also thank participants at the 37th Spring International Conference of the French Finance Association held at Audencia Business School France and the 10th International Conference of the Financial Engineering and Banking Society (FEBS) held at IAE Lille University School of Management France, for helpful comments and suggestions. We would like to thank the Editor-in-Chief Professor Christophe Godlewski and two anonymous referees for the helpful comments and suggestions which has helped us improve the paper. Any remaining errors are our own.

1. Introduction

Practical forecasting and theoretical financial models rely on an understanding of asset price volatility and the ways in which information propagates across markets. The seminal contributions of Engle et al. (1990) and Ito et al. (1992) regarding the information flow in currency markets introduce the concepts of heat waves and meteor showers.[1] Heat waves are associated with local autocorrelation structures, i.e. those specific to a trading market or a trading window, while meteor showers show evidence of dependence across markets (or trading windows).

Recently, Greenwood-Nimmo et al. (2016) examine and find spillovers among G10 currencies using an empirical network model on daily returns, the option-implied risk-neutral volatility and skewness. The work of Lahaye and Neely (2020), based on the earlier findings of Cai et al. (2008) on the role of jumps in driving volatility spillover, revisit the meteor shower and heat wave effects by decomposing the daily realized variance into continuous and jump components. They find both effects in the integrated volatility, however, meteor showers being more influential than heat waves. Su (2021) investigates the determinants of volatility spillovers in the FX market using an extended heterogeneous autoregressive (HAR) model incorporating market state. He finds that both meteor shower and heat wave effects are present. However, he argues that due to

1 The literature on exchange rates has evolved from an analysis of periodic patterns, scaling or long-memory properties, to the modelling of intra-daily and daily exchange rate returns (see, among many others, the works of Engle et al. (1990), Baillie and Bollerslev (1991), Hilliard and Tucker (1992), Dacorogna et al. (1993), Andersen and Bollerslev (1997), Guillaume et al. (1997), and Muller et al. (1997)).

global trading and correlated common shocks, the meteor shower effect dominates over heat waves.

Our work contributes to the stream of empirical literature on forex markets in several ways. Barunik et al. (2017) analyse the asymmetry in the forex market semivariances using forecast error variance decomposition, building on the recent stock market evidence which shows differences in the roles of good and bad volatility (Patton and Sheppard, 2015). So firstly, we evaluate the impact of good versus bad volatility on the evolution of the volatility of several clusters of exchange rates with respect to selected leading currencies, namely the US Dollar, the Euro, the UK Pound and the Japanese Yen. These currencies represent a large fraction of exchange rate trades, approximately 75% of average daily turnover (BIS, 2019).[2] From a methodological point of view, unlike common time series setting as in Lahaye and Neely (2020), and Su (2021), we adopt a panel approach. Our analyses highlight differences across exchange rate panels that are attributable to the reference leading currency. In addition, as we use data recorded at high frequency and on a 24-hour basis, we are also able to track how the impact of good and bad volatility changes across time zones. For a given currency, different behaviours across time zones might be associated with the local relevance of a given leading currency, complementing the analyses made across leading currencies.

Our second research direction focuses on the role of jumps in currencies. We deviate from Patton and Sheppard (2015) while identifying the discontinuous component of exchange rate evolution, a choice that allows the direct ex-post evaluation of jump signs. In this respect, we pre-test the series for jumps, decompose continuous part of good and bad volatility after removing the returns associated with jumps, and separate positive and negative jumps. We evaluate the impact of signed jumps on the currencies by differentiating between the leading currencies and the time zones. With respect to these first two issues, we expect to identify differences in the behaviours of our currency baskets over time zones. In fact, leading currencies might be more relevant over a specific time zone, while the impact of signed variations could differ across time zones as well as over leading currencies. To complement these two findings, we take a forecasting perspective and evaluate the impact of signed variations, focusing over increasing horizons to highlight possible differences over time

2 Triennial Central Bank Survey. Foreign exchange turnover in 2019. Bank for International Settlements.

zones, across currencies, for different components of the exchange rate volatility, accounting for the sign.

While the previous elements focus on the descriptive features of the forex market, our analyses also focus on the economic interpretation of our findings, in particular we consider the interdependence across trading periods. We thus analyse the interdependence across time zones, verifying whether, for a given leading currency basket, the information associated with specific time zones is dominant in the evolution of the volatility. Therefore, we contribute to the literature using a framework closely related to that of Lahaye and Nelly (2020), but with two relevant differences. Firstly, building on the work of Patton and Sheppard (2015), we disentangle the role of "good" and "bad" volatility. This allows us to evaluate the contribution to heat waves and/or meteor showers associated with positive and negative returns. Moreover, by using a similar interpretation, and making use of a procedure that allows us to separate jumps into positive and negative, we account for the jump sign effect. Notably, when recovering the good and bad volatility components, we introduce a criterion to identify, within each time zone, which is the riskier currency in each exchange rate; which is associated with the construction of a coherent modelling strategy. As a final analysis, we evaluate the horizon effect and determine the role of signed volatilities and jumps in driving the future evolution of the realized volatility, again from the angle of heat waves and meteor showers.

The estimates of the classic heteroskedastic auto-regressive (HAR) specification confirm the strong presence of heat waves, in line with the autocorrelation structure that characterizes the realized volatility sequences. Extending the model to dependence across time zones, meteor shower effects appear. They are quite diffuse when focusing on statistical significance, but when we account for their strength, it emerges they are stronger for contemporaneous European and US trading activity on the subsequent trading in US markets only, and then from the US market to the following Asian market trading. We might interpret this in light of the activeness of the European and US markets. We decompose the volatility into good and bad components, and cluster assets in such a way that shocks hitting the riskier currency in an exchange rate lead to good volatility. We observe that heat waves are stronger for good volatility than bad volatility. Furthermore, meteor showers are much more diffused for good volatility, but we do observe some heterogeneity across the leading

currencies. The jump component of the volatility, in line with the existence of heat waves, only influence the future volatility of the time zones where they originate. This evidence is somewhat unexpected as it appears that jumps on day t in time zone i impact the realized volatility on day $t+1$ in time zone i but do not have any effect on the realized volatility of the same day in time zone $i+1$. Therefore, only local jumps are relevant in driving the evolution of the zone-specific realized volatility. For the horizon effect, heat waves are clearly present but the asymmetric role of good and bad volatility is confirmed only over a short-term horizon. Meteor showers are present and their strength is in line with the previous analyses.

The paper proceeds as follows. In Section 2 we describe the data and the estimators we adopt for disentangling the continuous and discontinuous components of the exchange rate volatility while preserving the information of the sign, and we introduce the modelling strategy including the parameter estimators. Section 3 presents our empirical findings in subsections associated with the four research lines. Section 4 concludes.

2. Data description & Model

The data we use for empirical analysis consists of high-frequency 5-minute exchange rate quotes against four major currencies, the US Dollar (USD), Euro (EUR), UK Pound (GBP) and Japanese Yen (JPY) from October 1, 2009 to September 30, 2020. After removing the pegged currency cases and time series with longer than two months' stale prices, our final sample comprises 19 FXs against USD, GBP and JPY and 17 against EUR. Table 1 shows the selected exchange rates for the four reference currencies. The start date is dictated by the trade-off between the number of currency pairs and a common sample for all pairs. All exchange rates are taken from the Kibot.com[3] database on a nearly 24-hour basis, so in a given day there are 288 prices with matched date/time information set at New York time.[4]

3 This data provider is lesser known than competitors, but its data quality is comparable to that of the New York Stock Exchange's TAQ database. A limited comparison of the two databases is available upon request.

4 For what concerns the treatment of the daylight saving, given that it is not coordinated and homogeneous on a global scale, we set it according to the standard use in the Eastern Time zone (ET), i.e., in New York time. Therefore, daylight saving is introduced in the data when considering its deviation with respect to Coordinated Universal Time (UTC), i.e., data are 5 hours behind UTC in autumn/winter and 4 hours behind UTC in spring/summer.

Table 1: Composition of the exchange rate database

			Reference currencies			
S. No.	**Symbol**	**Country and Currency**	**USD**	**EUR**	**GBP**	**JPY**
1.	AUD	Australia Dollar	X	X	X	X
2.	CAD	Canada Dollar	X	X	X	X
3.	CHF	Switzerland Franc	X	X	X	X
4.	CZK	Czech Republic Koruna	X	X	X	X
5.	DKK	Denmark Krone	X	X	X	X
6.	EUR	Euro Member Countries	X		X	X
7.	GBP	British Pound	X	X		X
8.	HUF	Hungary Forint	X	X	X	
9.	ILS	Israel Shekel	X	X	X	X
10.	INR	India Rupee		X	X	X
11.	JPY	Japan Yen	X	X	X	
12.	KRW	South Korea Won	X			X
13.	MXN	Mexico Peso	X	X	X	X
14.	MYR	Malaysian Ringgit	X		X	X
15.	NOK	Norway Kroner	X	X	X	X
16.	NZD	New Zealand Dollar	X	X	X	X
17.	PLN	Poland Zloty	X	X	X	X
18.	RUB	Russia Rouble	X		X	X
19.	SEK	Sweden Krona	X	X	X	X
20.	TRY	Turkish New Lira	X	X	X	X
21.	USD	USA Dollar		X	X	X
Total pairs			**19**	**17**	**19**	**19**

Note: the tables reports the exchange rates included in our dataset.

We focus on the price volatility of four time zones so we utilize all the 24-hour data set, splitting the day trades into four samples, as detailed below. From our analysis we exclude the transactions executed from 18:00 Friday to 18:00 Sunday NY time, because of the low activity on these days, which could bias our analyses. We denote the observed log-prices on a given trade day as $p_0, p_1, \ldots, p_n$ where $n+1$ is the number of unique time stamps between 0:00:00 and 24:00:00 that have prices.

The time zones capture the trading activity in a particular region/location. Consequently, taking into account the timing of our data (set to New York time), we select the time zones of day t as follows: from 18:00 of day (t-1) to 02:55 of day t we have 108 observations associated with trading in Tokyo and Sydney; the sample from 03:00 of day t to 07:55 of day t includes 60 observations associated with trading in London only; from 08:00 of day t to 11:55 of day t we have 48 observations associated with trading in London and NY jointly; and finally, from 12:00 of day t to 17:55 of day t we recover 72 observations associated with trading in NY (and US) only. See **Figure 1** for a graphical representation of our time zone structure. Note that the trading zones we consider make a balance between trading activity and the need for including in each time zone a sufficient number of data points to build a time-zone specific model. Consequently, our time zones slightly differ from those adopted by other studies, such as Melvin and Melvin (2003), Cai et al. (2008) and Lahaye and Neely (2020). The most relevant difference is the use of four time zones instead of the five adopted by, for instance, Cai et al. (2008). We note that the missing time zone (or trading segment) corresponds to what the previously cited papers associate with the joint trading in Asia and Europe. However, this trading segment lasts only one hour, and thus has limited information content for subsequent analyses or for recovering realized volatility and identifying the occurrence of jumps. In the following, we indifferently use time zones or trading segments to identify the four periods into which we separate a trading day. Moreover, we refer to the trading we associate with the London market as trading zone 1 and the trading associated with the overlap in trading between Europe and North America as trading zone 2. Trading zones 3 and 4 refer to the trading in North America only and in the Australia-Asia area, respectively.

Using the 5-minutes data and focusing on the entire day, we filter the intra-daily periodic component following Boudt, Croux and Laurent (2011). Then, on the filtered data, we work on a time-zone basis and compute the following quantities: the realized volatility $RV_t^{(j)}$ (j identifies the time zone and t refers to a given day), an estimate of the daily total variation; the daily jumps and signed (positive and negative) jumps, $\Delta J_t^{2,(j)}$, $\Delta J_t^{2+,(j)}$, $\Delta J_t^{2-,(j)}$, with $\Delta J_t^{2,(j)} = \Delta J_t^{2+,(j)} + \Delta J_t^{2-,(j)}$, which estimate the daily discontinuous component of the total variation – jumps are identified at the intra-daily level with the test put forward by Lee and

Figure 1: Time zones as per trading activities

Note: From 18:00 of day (t-1) to 02:55 of day t, 108 observations associated with trading in Tokyo and Sydney. From 03:00 of day t to 07:55 of day t, 60 observations associated with trading in London only. From 08:00 of day t to 11:55 of day t, 48 observations associated with trading in London and NY jointly. From 12:00 of day t to 17:55 of day t, 72 observations associated with trading in NY only. The returns at a specific time period are based on price at that time and previous period price and thus a five-minute interval is left blank for clarity between the time zones.

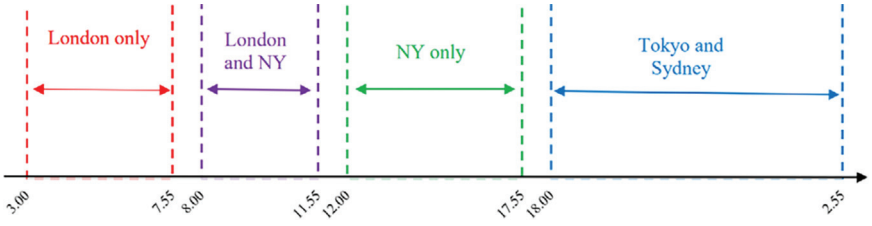

Mykland (2008); the *Good* and *Bad* volatility, $RS_t^{+,(j)}$ and $RS_t^{-,(j)}$, estimating the continuous contribution to the total variation. We note that $RV_t^{(j)} = RS_t^{+,(j)} + RS_t^{-,(j)} + \Delta J_t^{2,(j)}$. Details on the computation of the various quantities are included in Appendix A.

A preliminary descriptive analysis, see Appendix B, highlights the existence of heterogeneity among leading currencies and time zones. This suggests that the analysis of the dynamic volatility might also be heterogeneous among time zones and leading currencies. This aspect is analysed in the following Section 3.

In analysing the role of good and bad volatilities and signed jumps for predictability of exchange rate total realized volatility, over and across time zones, we use variations of the popular heterogeneous autoregression (HAR) model (Corsi, 2009; Müller et al., 1997). The standard HAR, in general, regresses the realized variance (RV) on three indicators built from lagged RVs, i.e., the 1-day lag, the average of the last 5 days, and the average over the last 22 days. For interpretation purposes, and coherently with Patton and Sheppard (2015), we use a re-parameterization of the HAR model which is numerically identical (in terms of fit to the data) to the original specification of Corsi (2009). In our model, the 2nd term is based only on the average realized variances between the 2 and 5 day lags, and the 3rd term comprises only the realized variances between the 6 and 22 day lags:

$$\bar{y}_{h,t+h} = \mu + \phi_d y_t + \phi_w \left(\frac{1}{4} \sum_{i=1}^{4} y_{t-i} \right) + \phi_m \left(\frac{1}{17} \sum_{i=5}^{21} y_{t-i} \right) + \epsilon_{t+h} \quad (1)$$

where y is RV for a specific time horizon, and $\bar{y}_{h,t+h} = \frac{1}{h} \sum_{i}^{h} y_{t+i}$ is the h-day average cumulative volatility. Hereafter, we use $\bar{y}_{w,t}$ to denote the average value over lags 2 to 5 and $\bar{y}_{m,t}$ indicates the mean value between 6 and 22 days lag. The model allows us to evaluate the impact of the daily, weekly and monthly volatility proxies on the total volatility at time $t+h$, where $h>0$ represents a forecast horizon. We note that we refer to the weekly and monthly proxies for simplicity but these are in reality representing the weekly impact going beyond the daily impact and the monthly effect going beyond the weekly effect. In the following, we extend the HAR model by introducing in the dynamic additional elements, associated with asymmetry, signed components and interdependence between time zones. In all cases, we estimate the various models for forecast horizons ranging from $h=1$ to 66 days, similarly to Patton and Sheppard (2015), from which we also borrow the estimation approach (see Appendix C for details).

In the following, we first focus on the serial dependence structure within each trading segment (time zone) highlighting the relevance and impact of specific features of the data, and then focus on the existence of meteor showers and heat waves within our dataset.

3. Empirical results

3.1 The HAR model results

Our first model corresponds to a baseline heterogeneous autoregressive model of Corsi (2009) augmented by the introduction of asymmetry, an additional component adopted in several empirical works; see, among others, Corsi and Renò (2012), and, in a different framework, Ning et al. (2015). We adopt here the same asymmetric specification of Patton and Sheppard (2015). Hence, we estimate the following specification:

$$\overline{RV}_{h,i,t+h} = \mu + \phi_d RV_{i,t} + \gamma RV_{i,t} I_{\left[r_{i,t}<0\right]} + \phi_w \overline{RV}_{w,i,t} + \phi_m \overline{RV}_{m,i,t} + \epsilon_{i,t+h} \quad (2)$$

where $\overline{RV}_{h,i,t+h}$, $\overline{RV}_{w,i,t}$ and $\overline{RV}_{m,i,t}$ have already been defined in Eq. (1), while $I_{[r_{i,t}<0]}$ is an indicator of negative lagged daily FX returns. We estimate the models parameters with a fixed effect estimator, for each cluster of currencies (with respect to the leading currencies) and for each time zone. This baseline specification helps us to analyse the heat wave presence. To examine meteor showers across regions, we estimate the following extended specification:

$$\overline{RV}_{i,l,h,t+h} = \mu + \sum_{j=1}^{4}\left(\phi_{j,d} RV_{j,l,t-j\Delta t}\right) + \gamma RV_{i,l,t} I_{[r_{i,l,t}<0]} + \phi w\overline{RV}_{i,l,w,t} + \phi_m \overline{RV}_{i,l,m,t} + \epsilon_{i,t+h} \quad (3)$$

where we allow the volatility of exchange rate i in time zone l to depend on the volatilities of the same exchange rate observed in the same time zone and in the previous three time zones. For instance, if we focus on the USD currency panel, and on the USD/EUR exchange rate in time zone 3, the volatility for time zone 3 and day t+1, depends on the volatility of time zone 3 at day t, the volatility of time zones 2 and 1 at day t, and the volatility of time zone 4 at day t-1.

Table 2A-D gives the results for the selected leading currency (we always exclude the intercept). In each time zone, we report results for basic as well as extended HAR specifications. We evaluate the presence of heat waves and meteor shower combining the statistical significance of coefficients with their size. In the USD case (Panel A), the baseline model shows heterogeneity across the active geographical areas. The coefficients of the daily lag range from 0.217 to 0.338, with the lowest value associated with the third (NY only) time zone. Furthermore, there is no evidence of asymmetry as the coefficients of the asymmetric term are not significant at the 1% level, and only in two time zones do we have significant coefficients but at the 5% level. For the extended HAR, consecutive time zones have a statistically significant impact on the volatility of any particular time zone. However, a significantly higher (0.186) spillover is evident from time zone 2 (London and NY) to time zone 3 (NY only). Similarly, a significant and high (0.177) influence of volatility from time zone 3 (NY only) to time zone 4 (Tokyo and Sydney) is noted.

For the Euro, Pound and Yen, the results of the basic and extended HAR are similar to USD i.e., low coefficient of daily lag in time zone 3

Table 2: The HAR specification with asymmetric effect

$$\overline{RV}_{h,t+h} = \mu + \phi_d RV_t + \gamma RV_t I_{[r_t<0]} + \phi_w RV_{w,t} + \phi_m RV_{m,t} + \epsilon_{t+h}$$

A. Estimation results for the USD

	ϕ_d^{TZ1}	ϕ_d^{TZ2}	ϕ_d^{TZ3}	ϕ_d^{TZ4}	γ	ϕ_w	ϕ_m	*Adj.* R^2
	0.338				−0.038	0.364	0.229	0.211
TZ=1	(16.07)				(−2.12)	(18.94)	(11.99)	
(London only)	**0.290**	*0.058*	*0.043*	0.006	−0.038	0.335	0.205	0.260
	(14.26)	(6.24)	(3.14)	(1.44)	(−2.11)	(17.35)	(10.48)	
		0.299			−0.039	0.332	0.305	0.202
TZ=2		(15.53)			(−2.25)	(15.98)	(14.48)	
(London and NY)	*0.047*	**0.266**	*0.034*	0.002	−0.038	0.314	0.291	0.226
	(3.67)	(13.36)	(2.70)	(0.79)	(−2.22)	(14.91)	(13.78)	
			0.217		−0.027	0.341	0.322	0.101
TZ=3			(10.42)		(−1.29)	(15.02)	(13.21)	
(NY only)	0.041	**0.186**	**0.149**	*0.021*	−0.013	0.254	0.228	0.200
	(1.49)	(8.25)	(7.87)	(4.38)	(−0.70)	(10.86)	(8.94)	
				0.290	−0.001	0.437	0.255	0.435
TZ=4				(13.91)	(−0.03)	(10.05)	(7.79)	
(Tokyo and Sydney)	0.022	*0.046*	**0.177**	**0.225**	0.003	0.368	0.201	0.484
	(1.29)	(3.65)	(5.33)	(10.12)	(0.15)	(9.77)	(5.39)	

B. Estimation results for the EUR

	ϕ_d^{TZ1}	ϕ_d^{TZ2}	ϕ_d^{TZ3}	ϕ_d^{TZ4}	γ	ϕ_w	ϕ_m	*Adj.* R^2
	0.320				−0.019	0.370	0.253	0.158
TZ=1	(15.47)				(−1.34)	(19.03)	(13.57)	
(London only)	**0.305**	*0.022*	*0.009*	0.001	−0.019	0.363	0.248	0.171
	(14.70)	(2.65)	(3.20)	(1.30)	(−1.32)	(18.76)	(13.26)	
		0.284			−0.042	0.334	0.295	0.067
TZ=2		(14.82)			(−2.41)	(15.19)	(11.52)	
(London and NY)	*0.095*	**0.231**	0.032	−0.001	−0.040	0.299	0.274	0.074
	(6.60)	(11.44)	(1.62)	(−0.69)	(−2.34)	(13.71)	(10.51)	
			0.190		−0.047	0.442	0.233	0.050
TZ=3			(10.60)		(−2.85)	(19.32)	(11.58)	
(NY only)	*0.081*	**0.257**	**0.117**	0.000	−0.032	0.313	0.146	0.109
	(4.51)	(7.71)	(7.56)	(0.09)	(−2.08)	(14.70)	(7.10)	
				0.255	−0.001	0.312	0.272	0.025
TZ=4				(11.75)	(−0.08)	(8.89)	(9.50)	
(Tokyo and Sydney)	*0.072*	0.035	**0.382**	**0.134**	−0.004	0.199	0.181	0.066
	(2.07)	(1.01)	(4.19)	(5.52)	(−0.22)	(6.68)	(5.19)	

Table 2 (Continued)**:** The HAR specification with asymmetric effect

C. Estimation results for the GBP

	ϕ_d^{TZ1}	ϕ_d^{TZ2}	ϕ_d^{TZ3}	ϕ_d^{TZ4}	γ	ϕ_w	ϕ_m	*Adj.* R^2
TZ=1 (London only)	**0.300** (10.48)				−0.034 (−1.76)	0.366 (16.48)	0.249 (10.96)	0.350
	0.233 (7.71)	**0.102** (4.23)	*0.072* (3.59)	0.013 (1.98)	−0.038 (−1.97)	0.321 (13.51)	0.219 (9.55)	0.358
TZ=2 (London and NY)		**0.257** (14.80)			0.005 (0.24)	0.401 (16.44)	0.244 (10.59)	0.212
	0.078 (3.46)	**0.208** (10.97)	*0.034* (3.47)	0.007 (1.10)	0.003 (0.18)	0.363 (14.15)	0.222 (9.37)	0.219
TZ=3 (NY only)			**0.206** (8.45)		−0.036 (−1.67)	0.377 (15.35)	0.288 (11.99)	0.119
	0.016 (0.50)	**0.315** (2.75)	**0.131** (5.21)	0.013 (1.80)	−0.016 (−0.84)	0.244 (6.20)	0.192 (5.69)	0.366
TZ=4 (Tokyo and Sydney)				**0.254** (9.26)	0.026 (0.60)	0.465 (6.10)	0.245 (7.17)	0.290
	0.025 (1.24)	0.022 (1.19)	**0.281** (4.92)	**0.172** (5.02)	0.038 (0.86)	0.366 (5.86)	0.198 (5.30)	0.352

D. Estimation results for the JPY

	ϕ_d^{TZ1}	ϕ_d^{TZ2}	ϕ_d^{TZ3}	ϕ_d^{TZ4}	γ	ϕ_w	ϕ_m	*Adj.* R^2
TZ=1 (London only)	**0.339** (14.73)				−0.047 (−2.27)	0.385 (15.57)	0.235 (10.68)	0.233
	0.266 (12.39)	*0.058* (4.62)	*0.094* (7.37)	0.004 (1.12)	−0.041 (−2.10)	0.337 (14.02)	0.205 (9.44)	0.272
TZ=2 (London and NY)		**0.331** (12.64)			−0.030 (−1.52)	0.359 (14.23)	0.265 (11.17)	0.395
	0.053 (3.82)	**0.262** (10.82)	*0.090* (5.72)	0.008 (1.71)	−0.026 (−1.41)	0.318 (12.35)	0.233 (9.77)	0.416
TZ=3 (NY only)			**0.311** (8.12)		−0.041 (−1.42)	0.362 (15.44)	0.277 (11.42)	0.301
	0.043 (1.52)	**0.249** (8.95)	**0.212** (6.35)	*0.026* (2.91)	−0.036 (−1.34)	0.238 (8.84)	0.178 (6.85)	0.385
TZ=4 (Tokyo and Sydney)				**0.370** (9.76)	−0.122 (−3.26)	0.429 (9.94)	0.223 (8.10)	0.292
	0.050 (1.26)	−0.005 (−0.09)	**0.543** (3.24)	**0.220** (6.19)	−0.103 (−3.19)	0.285 (6.57)	0.142 (4.45)	0.366

Note: The model is the reference model that uses realized variance and an asymmetric term. These summary results are for the forecast horizon of one day. In all cases, average values of R^2 for individual currencies are reported. The robust t-statistics are in parentheses. We report in bold daily realized volatility coefficients which are statistically significant and larger than 0.1; smaller and statistically significant coefficients are in italics.

(NY only). In the case of Yen, the highest daily lag coefficient is found in time zone 4 (Tokyo and Sydney). The asymmetric terms are almost always insignificant, at the 1% level of significance. The influence across time zones is also like USD. A significantly higher influence is evident from time zone 2 (London and NY) to time zone 3 (NY only) and from time zone 3 (NY only) to time zone 4 (Tokyo and Sydney). For the Pound, a higher impact of lagged RV in time zone 2 (London and NY) to time zones 1 (London only) is also noted.

These results collectively show evidence of heat waves in all time zones, an expected result given the known serial dependence characterizing realized volatility sequences. When we augment the model with impact across time zones, meteor showers appear. They tend to be quite diffused if we focus only on the statistical significance. However, if we also take into account the coefficient size, we note that meteor showers are stronger from time zone 2 to 3 and from time zone 3 to 4. We might read this in light of the relevance of these time zones within the global financial markets. Moreover, the information spillover from the joint European and US trading zone to the US trading zone might be related to the presence of US-based agents active in both time zones. For the link between the US time zone and the Asian time zone, we might also read this in light of the accumulation of information within a calendar day, which impacts the following day's exchange rates in the first time zone trading, i.e. the Asian zone.

The adjusted R-square values are higher in the case of the extended HAR specification compared to the basic HAR, which indicates that future volatility of a specific time zone is also explained by the volatility in other time zones. We plot the adjusted R-square values of the HAR model estimations for individual currencies in **Figure 2** (Panels A to D for the four leading currencies). Apparently, the explanatory power of individual HAR models is relatively lower when FX are quoted against GBP. Generally, adjusted R-square values are higher in time zones 1 and 2, with few exceptions. Also, other currencies, such as ILS and INR, have lower values, irrespective of the leading currencies.

3.2 The role of signed realized semivariances and signed jumps

Next, we examine the role of signed realized semivariances in driving the future volatility of exchange rates across time zones and therefore we estimate the following basic and extended specifications:

Figure 2: R-squared values of individual currencies for time zones

Note: For each leading currency, we report the adjusted r-squared of the baseline HAR model. The x-axis shows the exchange rates, and each time zone adopts a different colour.

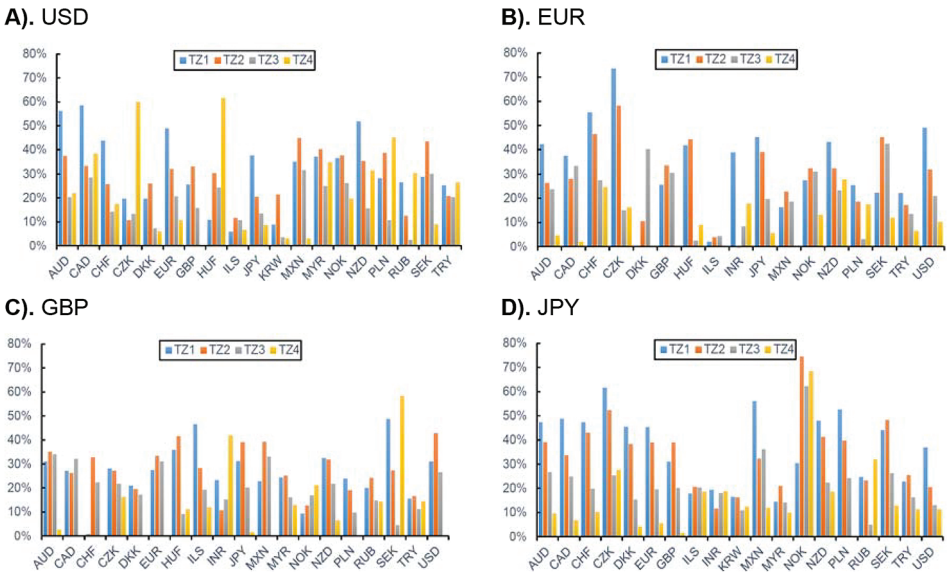

$$\overline{RV}_{h,i,t+h} = \mu + \boldsymbol{\phi_d^+ RS_{i,t}^+} + \boldsymbol{\phi_d^- RS_{i,t}^-} + \phi_J \Delta J_{i,t}^2 + \phi w \overline{RV}_{w,i,t} + \phi_m \overline{RV}_{m,i,t} + \epsilon_{i,t+h} \tag{4}$$

$$\overline{RV}_{i,l,h,t+h} = \mu + \sum_{j=1}^{4} \left(\phi_{j,d} \boldsymbol{RS}_{j,l,t-j\Delta t}^+ \right) + \sum_{j=1}^{4} \left(\phi_{j,d} \boldsymbol{RS}_{j,l,t-j\Delta t}^- \right) + \sum_{j=1}^{4} \left(\phi_{jJ} \Delta J_{j,l,t-j\Delta t}^2 \right) + \phi w \overline{RV}_{i,l,w,t} + \phi_m \overline{RV}_{i,l,m,t} + \epsilon_{i,t+h} \tag{5}$$

where the realized semivariances $RS_{i,t}^+$ and $RS_{i,t}^-$ are calculated as per Eq. (A.4) and jump variations $\Delta J_{i,t}^2$ according to Eq. (A.5). Other terms are equivalent to those in Eq. (2). In this model, we introduce the signed volatility along with the jump variation. We do not allow for returns asymmetry because it turns out to be only slightly significant in a few cases.

Notably, we realize that a preliminary transformation on the exchange rates is needed to estimate a pooled OLS with semivariances. In fact, while the realized volatility of, say, the EUR/USD exchange rate is identical to the realized volatility of the USD/EUR exchange rate, the good and bad volatility values, in a given day, are inverted. This is a consequence of using intra-daily log-returns characterised by equal values for EUR/USD and USD/EUR but with opposite signs. Consequently, in order to obtain a coherent set of results in the panel estimate, we have to specify for each exchange rate which version, direct or indirect, is used, taking the point of view of an investor located in the country of the leading currency we are considering. We chose a relatively simple criterion, that builds on the expectation of observing a larger impact of bad volatility (i.e. negative shocks), as opposed to good volatility, on the realized volatility, coherent with the results of Patton and Sheppard (2015). However, focusing on exchange rates, the identification of negative shocks depends on the version of the exchange rate considered. As an example, consider a US investor, and take the indirect exchange rate between, say, the USD and the Euro, i.e. we evaluate the volume of Euro for 1 USD. A negative shock on the Euro leads to a depreciation of the Euro against the USD and, consequently, an increase of the Euro volume for 1 USD. Therefore, a negative shock equals a positive return on the USD/EUR exchange rate. On the contrary, if we take the direct exchange rate, i.e. the USD price of 1 Euro, a negative shock on the Euro turns into a negative return on the exchange rate. Consequently, in the indirect case, shocks on the local currency correspond to negative returns and thus contribute to bad volatility while shocks on the foreign currency contribute to good volatility. In this setting, the largest between the good and bad volatility can be used to identify which is the riskiest currency in the exchange rate. In our analyses we denote as the riskiest currency the one with the largest contribution coming from negative shocks. Continuing with our example, if the Euro is riskier than USD, and thus negative shocks on the Euro are more relevant than positive shocks on the Euro, we expect the good volatility to be higher than the bad volatility (keep in mind we use indirect rates and negative shocks on the USD to correspond to drops in the exchange rate and thus contribute to the bad volatility).

Given the previous discussion, in each time zone, for each leading currency and for each exchange rate, we estimate a univariate HAR model with lagged semivariances for the indirect exchange rate (i.e. the volume of

foreign currency for one unit of the leading currency). If the coefficient of the good volatility is higher than the coefficient of the bad volatility, it means that the foreign currency is riskier than the leading currency, and thus we keep the indirect rate. If the leading currency is riskier, we revert the exchange rate to its direct form. Note that this puts on the same side the currencies that are perceived by the market to be riskier in a specific time zone. The criteria we use are clearly data-driven and deliberate, but make the exchange rates adopted in the model coherent with respect to market perception of currency risk. To the best of our knowledge, such an ordering criterion for exchange rates is novel and has never been used in previous studies. Table D.2 in the appendix lists the versions of the exchange rates we adopt in each time zone.

In **Table 3**, we report the results for selected coefficients, excluding the intercept and the coefficients associated with the weekly and monthly lags (which are always significant and coherent with the relevance of the heat wave effect). We skip the coefficients of jump variations, as the results of the model with continuous and jump specifications are provided in the appendix.

Overall, we note a significant asymmetry between the coefficients of positive and negative semivariances, consistent with the findings of Patton and Sheppard (2015); we stress that, given the discussion above, we do expect a larger coefficient for good volatility. This shows that the heat wave effect is mostly driven by shocks on the riskier currency entering the exchange rates.

For USD and EUR, meteor showers are only present in cases of positive semivariances, i.e. for shocks originating from the riskier currencies. In the case of GBP, negative semivariance in time zone 2 impacts time zone 3 and time zone 3 impacts time zone 4. In the case of JPY, meteor showers effect exits for both positive and negative semivariances. Again, where positive or negative semivariances are present, the meteor shower effect is significant from time zone 2 to 3 and from time zone 3 to 4. The estimates of basic specifications for individual currencies are shown in **Figure 3** and indicate asymmetry in the effect of signed semivariances, without patterns we could associate with the time zones or leading currencies. Therefore, while the use of semivariances confirms the relevance of the meteor showers effect, on the economic sides we do not identify important insights associated either to the time-zone specificities or to the currency at which we are pointing (between USD, EUR, GBP and JPY).

Table 3: The role of realized semivariances

$$\overline{RV}_{h,t+h} = \mu + \boldsymbol{\phi_{C+}RS_t^+} + \boldsymbol{\phi_{C-}RS_t^-} + \phi_J J_t + \phi_w RV_{w,t} + \phi_m RV_{m,t} + \epsilon_{t+h}$$

A. Estimation Results for the USD

	ϕ_{C+}^{TZ1}	ϕ_{C+}^{TZ2}	ϕ_{C+}^{TZ3}	ϕ_{C+}^{TZ4}	ϕ_{C-}^{TZ1}	ϕ_{C-}^{TZ2}	ϕ_{C-}^{TZ3}	ϕ_{C-}^{TZ4}	*Adj.* R^2
TZ=1 (London only)	**0.543** (13.95)				**0.253** (8.73)				0.214
	0.464 (12.28)	**0.121** (5.38)	*0.064* (2.01)	−0.014 (−0.32)	**0.181** (6.25)	*0.056* (3.12)	*0.058* (2.01)	0.041 (0.78)	0.266
TZ=2 (London and NY)		**0.448** (12.65)				**0.284** (9.59)			0.203
	0.079 (2.49)	**0.386** (10.81)	*0.052* (2.60)	0.011 (1.24)	*0.078* (2.09)	0.232 (7.69)	0.028 (1.33)	−0.005 (−0.60)	0.233
TZ=3 (NY only)			**0.344** (8.82)				**0.208** (7.65)		0.101
	0.089 (2.33)	**0.105** (3.14)	**0.291** (7.82)	0.008 (0.40)	0.034 (1.06)	0.012 (0.43)	**0.160** (5.86)	0.043 (1.92)	0.210
TZ=4 (Tokyo and Sydney)				**0.476** (7.42)				**0.204** (4.20)	0.436
	0.148 (3.44)	*0.065* (2.59)	**0.213** (3.67)	**0.366** (7.59)	0.006 (0.14)	0.020 (1.14)	0.121 (1.69)	**0.123** (2.11)	0.480

B. Estimation Results for the EUR

	ϕ_{C+}^{TZ1}	ϕ_{C+}^{TZ2}	ϕ_{C+}^{TZ3}	ϕ_{C+}^{TZ4}	ϕ_{C-}^{TZ1}	ϕ_{C-}^{TZ2}	ϕ_{C-}^{TZ3}	ϕ_{C-}^{TZ4}	*Adj.* R^2
TZ=1 (London only)	**0.484** (11.14)				**0.305** (9.82)				0.175
	0.380 (8.40)	**0.118** (2.40)	**0.156** (2.56)	−0.003 (−0.90)	**0.225** (6.45)	0.152 (1.77)	0.004 (0.15)	0.003 (0.83)	0.200
TZ=2 (London and NY)		**0.471** (7.81)				**0.222** (6.25)			0.067
	0.180 (4.43)	**0.385** (6.62)	0.057 (1.79)	−0.001 (−0.08)	**0.107** (2.22)	**0.132** (3.76)	0.029 (1.64)	0.001 (0.13)	0.077
TZ=3 (NY only)			**0.357** (8.66)				**0.168** (4.21)		0.051
	0.097 (3.67)	**0.118** (3.40)	**0.281** (7.33)	−0.009 (−0.51)	0.059 (2.91)	0.062 (2.45)	**0.125** (3.22)	0.023 (1.63)	0.136
TZ=4 (Tokyo and Sydney)				**0.488** (5.85)				**0.170** (2.20)	0.025
	0.187 (1.81)	−0.070 (−1.24)	**0.488** (1.74)	**0.295** (5.05)	0.071 (2.32)	−0.056 (−0.82)	**0.648** (2.33)	−0.017 (−0.18)	0.044

Table 3 (Continued)**:** The role of realized semivariances

C. Estimation Results for the GBP

	ϕ_{C+}^{TZ1}	ϕ_{C+}^{TZ2}	ϕ_{C+}^{TZ3}	ϕ_{C+}^{TZ4}	ϕ_{C-}^{TZ1}	ϕ_{C-}^{TZ2}	ϕ_{C-}^{TZ3}	ϕ_{C-}^{TZ4}	*Adj.* R^2
TZ=1 (London only)	**0.467** (9.17)				**0.296** (8.80)				0.345
	0.364 (6.68)	*0.090* (2.12)	**0.151** (3.12)	0.033 (1.92)	**0.179** (4.56)	**0.186** (2.23)	*0.090* (2.10)	−0.009 (−0.53)	0.359
TZ=2 (London and NY)		**0.415** (10.11)				**0.259** (9.93)			0.220
	0.048 (1.19)	**0.319** (8.63)	**0.111** (3.53)	−0.014 (−1.05)	0.172 (1.83)	**0.174** (5.68)	*0.042* (2.30)	0.009 (0.56)	0.227
TZ=3 (NY only)			**0.379** (8.99)				**0.199** (6.40)		0.121
	0.070 (2.27)	*0.089* (2.33)	**0.316** (7.91)	−0.010 (−0.40)	0.012 (0.49)	**0.143** (2.71)	**0.145** (4.73)	0.035 (1.34)	0.377
TZ=4 (Tokyo and Sydney)				**0.463** (7.98)				**0.162** (3.44)	0.291
	0.101 (1.47)	0.005 (0.14)	**0.406** (3.54)	**0.324** (8.41)	−0.012 (−0.77)	−0.023 (−0.39)	**0.438** (2.95)	0.029 (0.42)	0.368

D. Estimation Results for the JPY

	ϕ_{C+}^{TZ1}	ϕ_{C+}^{TZ2}	ϕ_{C+}^{TZ3}	ϕ_{C+}^{TZ4}	ϕ_{C-}^{TZ1}	ϕ_{C-}^{TZ2}	ϕ_{C-}^{TZ3}	ϕ_{C-}^{TZ4}	*Adj.* R^2
TZ=1 (London only)	**0.505** (12.83)				**0.303** (7.18)				0.235
	0.390 (10.77)	*0.093* (3.78)	**0.137** (5.56)	*0.037* (2.33)	**0.194** (4.63)	*0.083* (4.02)	**0.133** (5.44)	*-0.032* (−2.16)	0.277
TZ=2 (London and NY)		**0.532** (9.89)				**0.333** (10.40)			0.398
	0.137 (3.57)	**0.415** (8.54)	**0.127** (3.68)	0.024 (1.04)	*0.089* (2.42)	**0.227** (6.61)	**0.112** (4.60)	−0.014 (−0.69)	0.423
TZ=3 (NY only)			**0.436** (6.65)				**0.332** (7.43)		0.301
	0.129 (4.97)	**0.116** (2.94)	**0.358** (5.92)	0.387 (1.00)	0.267 (0.70)	0.419 (1.13)	**0.263** (6.86)	0.218 (0.69)	0.387
TZ=4 (Tokyo and Sydney)				**0.725** (5.85)				**0.325** (0.36)	0.291
	0.182 (2.21)	−0.574 (−0.69)	**0.944** (2.61)	**0.360** (4.12)	0.588 (0.44)	−0.347 (−0.62)	**0.794** (3.16)	−0.115 (−1.57)	0.377

Note: The model is an extended version of the basic HAR model where realized variance is decomposed into signed semivariances (continuous) and jump components. These summary results (skipped model co-efficient for jumps, lagged weekly and monthly RVs, as those are similar to values reported in Appendix) are for the forecast horizon of one day. In all cases, average values of adjusted R^2 for individual currencies are reported. The robust t-statistics are in parentheses. In bold we highlight statistically significant coefficients larger than 0.1; smaller and statistically significant coefficients are in italics.

Figure 3: Asymmetric impact of positive and negative semivariances for individual currencies

Note: For each leading currency, we report on the x-axis the coefficient of the positive semivariances and on the y-axis the coefficient of negative semivariances. Each symbol refers to an exchange rate, and each time zone adopts a different colour.

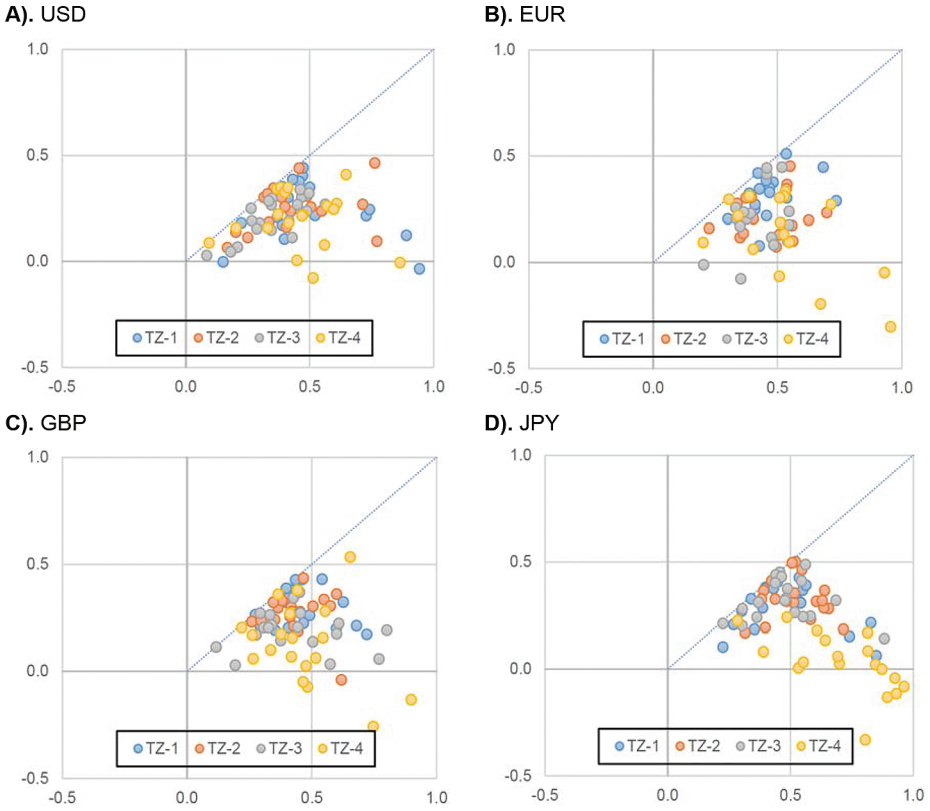

To further examine the impact of signed jump variations in driving the future volatility of exchange rates across time zones, we estimate the following basic and extended specifications:

$$\overline{RV}_{h,i,t+h} = \mu + \phi_d RV_{i,t} + \boldsymbol{\phi_{J^+}} \Delta \boldsymbol{J^{2+}_{i,t}} + \boldsymbol{\phi J^-} \Delta \boldsymbol{J^{2-}_{i,t}} + \phi_w \overline{RV}_{w,i,t} + \phi_m \overline{RV}_{m,i,t} + \epsilon_{i,t+h} \quad (6)$$

$$\overline{RV}_{i,l,h,t+h} = \mu + \sum_{j=1}^{4}\left(\phi_{j,d} RV_{j,l,t-j\Delta t}\right) + \sum_{j=1}^{4}\left(\phi_{j,J^+}\Delta \boldsymbol{J}^{2+}_{j,l,t-j\Delta t}\right) + \sum_{j=1}^{4}\left(\phi_{j,J^-}\Delta \boldsymbol{J}^{2-}_{j,l,t-j\Delta t}\right) + \phi w\overline{RV}_{i,l,w,t} + \phi_m\overline{RV}_{i,l,m,t} + \epsilon_{i,t+h} \quad (7)$$

where the realized variances $RV_{i,t}$ are calculated as per Eq. (A.3) and signed jump variations $\Delta \boldsymbol{J}^{2+}_{i,t}$ and $\Delta \boldsymbol{J}^{2-}_{i,t}$ according to Eq. (A.5). Other terms are equivalent to those in Eq. (3) and refer to the jumps observed in other time zones. By introducing these elements, we verify if also jumps are characterized by meteor showers and heat waves effects.

To summarize, the estimation results reported in **Table 4** indicate that the jumps (associated with both positive and negative returns) are only relevant in the time zones where they originate and indicate that jump variations have a heat wave effect. There is no significant difference between the impacts of signed jumps, which is also evident from the estimates of individual currencies shown in **Figure 4**. The meteor shower effect (impact of jumps across time zones in the extended model specifications) in both positive and negative signed jumps is present only from time zone 3 to 4, in the case of USD. For the other three leading currencies, this impact only occurs in the case of negative signed jumps. Overall, this evidence is a bit surprising as it implies that jumps affecting an exchange rate in day *t* and time zone *i* impact only the realized volatility of the same time zone but at day *t+1*, and there is no impact on the same day and time zone *i+1*. Therefore, jumps seem to have only a *local* impact. The information is conveyed by the continuous volatility component (total or with semivariances) only, given the evidence in the previous model estimates, and thus referring simply to the *predictable* component of the total variation. On the contrary, the jumps, the *unpredictable* component of the total variation, do have effect just within the time zone in which they appear, and are not transmitting to other time zones.

3.3 The horizon effect

So far we have examined the impact of signed semivariances on the volatility of next one day, and found asymmetries in their influence. In

Table 4: The role of realized jumps

$$\overline{RV}_{h,t+h} = \mu + \phi_C RVf_t + \boldsymbol{\phi_{J+} J_t^+} + \boldsymbol{\phi_{J-} J_t^-} + \phi_w RV_{w,t} + \phi_m RV_{m,t} + \epsilon_{t+h}$$

A. Estimation Results for the USD

	ϕ_{J+}^{TZ1}	ϕ_{J+}^{TZ2}	ϕ_{J+}^{TZ3}	ϕ_{J+}^{TZ4}	ϕ_{J-}^{TZ1}	ϕ_{J-}^{TZ2}	ϕ_{J-}^{TZ3}	ϕ_{J-}^{TZ4}	*Adj.* R^2
TZ=1 (London only)	**0.117** (3.68)				**0.132** (3.27)				0.214
	0.096 (3.00)	0.029 (1.65)	0.002 (0.13)	*-0.025* (−2.40)	**0.106** (2.70)	0.016 (0.97)	0.042 (1.42)	−0.004 (−0.90)	0.263
TZ=2 (London and NY)		**0.154** (4.32)				**0.123** (3.97)			0.205
	0.010 (0.87)	**0.142** (3.98)	0.034 (1.56)	−0.006 (−1.02)	0.016 (0.86)	**0.110** (3.57)	0.023 (1.01)	−0.002 (−0.91)	0.233
TZ=3 (NY only)			0.041 (1.22)				**0.109** (3.40)		0.101
	0.029 (1.05)	0.001 (0.03)	0.049 (1.46)	0.005 (0.27)	−0.042 (−2.31)	0.030 (1.00)	**0.111** (3.45)	−0.012 (−0.76)	0.209
TZ=4 (Tokyo and Sydney)				**0.217** (4.39)				*0.066* (2.04)	0.436
	−0.022 (−1.85)	0.028 (1.36)	**0.148** (2.30)	**0.203** (4.25)	−0.025 (−1.64)	0.053 (1.71)	**0.247** (4.67)	0.055 (1.77)	0.479

B. Estimation Results for the EUR

	ϕ_{J+}^{TZ1}	ϕ_{J+}^{TZ2}	ϕ_{J+}^{TZ3}	ϕ_{J+}^{TZ4}	ϕ_{J-}^{TZ1}	ϕ_{J-}^{TZ2}	ϕ_{J-}^{TZ3}	ϕ_{J-}^{TZ4}	*Adj.* R^2
TZ=1 (London only)	**0.112** (4.09)				*0.094* (3.13)				0.167
	0.066 (2.26)	*0.067* (2.83)	0.000 (0.04)	0.004 (1.89)	0.051 (1.64)	0.001 (1.14)	0.001 (0.69)	−0.002 (−0.81)	0.191
TZ=2 (London and NY)		*0.093* (2.81)				**0.154** (4.76)			0.066
	0.029 (1.67)	*0.071* (2.18)	−0.045 (−1.46)	0.008 (1.50)	0.000 (0.01)	**0.133** (4.25)	0.045 (1.35)	−0.014 (−2.11)	0.079
TZ=3 (NY only)			0.069 (1.52)				0.028 (1.45)		0.063
	0.006 (0.47)	0.008 (0.25)	0.069 (1.52)	−0.006 (−0.78)	0.008 (0.39)	0.007 (0.43)	0.026 (1.34)	−0.012 (−1.63)	0.157
TZ=4 (Tokyo and Sydney)				*0.085* (2.05)				0.039 (1.55)	0.027
	−0.007 (−0.44)	−0.021 (−0.49)	0.024 (0.18)	0.080 (1.97)	0.023 (0.58)	0.161 (1.80)	**0.234** (2.49)	0.027 (1.14)	0.047

Table 4 (Continued)**:** The role of realized jumps

C. Estimation Results for the GBP

	ϕ_{J+}^{TZ1}	ϕ_{J+}^{TZ2}	ϕ_{J+}^{TZ3}	ϕ_{J+}^{TZ4}	ϕ_{J-}^{TZ1}	ϕ_{J-}^{TZ2}	ϕ_{J-}^{TZ3}	ϕ_{J-}^{TZ4}	*Adj.* R^2
TZ=1 (London only)	**0.108** (3.69)				**0.130** (3.44)				0.345
	0.092 (3.21)	0.040 (1.10)	−0.003 (−0.24)	0.011 (0.89)	*0.098* (2.63)	0.018 (0.43)	0.040 (1.16)	0.000 (0.03)	0.359
TZ=2 (London and NY)		**0.158** (4.52)				**0.143** (4.69)			0.220
	0.069 (1.56)	**0.135** (3.91)	0.002 (0.26)	0.028 (1.43)	0.034 (0.90)	**0.112** (3.72)	*-0.019* (−2.11)	0.005 (0.29)	0.227
TZ=3 (NY only)			0.018 (1.10)				*0.073* (3.09)		0.120
	0.041 (1.85)	0.045 (0.72)	0.013 (0.79)	0.023 (1.05)	0.002 (0.11)	0.016 (0.34)	0.065 (2.80)	0.024 (0.81)	0.378
TZ=4 (Tokyo and Sydney)				**0.187** (4.31)				**0.118** (2.72)	0.290
	0.035 (2.29)	0.020 (0.74)	0.081 (1.61)	**0.176** (4.23)	0.039 (1.66)	−0.018 (−0.79)	**0.228** (2.05)	**0.126** (3.17)	0.365

D. Estimation Results for the JPY

	ϕ_{J+}^{TZ1}	ϕ_{J+}^{TZ2}	ϕ_{J+}^{TZ3}	ϕ_{J+}^{TZ4}	ϕ_{J-}^{TZ1}	ϕ_{J-}^{TZ2}	ϕ_{J-}^{TZ3}	ϕ_{J-}^{TZ4}	*Adj.* R^2
TZ=1 (London only)	**0.135** (5.34)				*0.084* (3.53)				0.235
	0.117 (4.75)	0.019 (0.78)	0.012 (0.66)	0.005 (0.49)	*0.057* (2.46)	−0.022 (−1.69)	*0.059* (2.20)	−0.007 (−0.64)	0.277
TZ=2 (London and NY)		**0.127** (3.81)				*0.085* (3.11)			0.397
	−0.004 (−0.30)	*0.073* (2.33)	*0.072* (2.60)	−0.004 (−0.40)	−0.011 (−0.87)	0.042 (1.58)	0.033 (1.57)	0.000 (0.02)	0.420
TZ=3 (NY only)			**0.812** (3.76)				**0.974** (3.72)		0.302
	−0.634 (−0.54)	−0.441 (−0.22)	**0.835** (3.22)	0.833 (0.48)	0.145 (0.93)	−0.400 (−1.96)	**0.963** (3.72)	0.275 (1.56)	0.386
TZ=4 (Tokyo and Sydney)				**0.220** (3.62)				0.687 (1.64)	0.292
	−0.198 (−1.45)	−0.165 (−1.38)	−0.144 (−0.13)	**0.184** (3.13)	−0.412 (−1.88)	−0.512 (−0.75)	**0.325** (2.17)	0.594 (1.43)	0.373

Note: The model is an extended version of the basic HAR model where realized variance is decomposed into its continuous and signed jump components. These summary results (skipped model co-efficient for continuous component, lagged weekly and monthly RVs, as those are similar to values reported in Table 3) are for the forecast horizon of one day. In all cases, average values of adjusted R^2 for individual currencies are reported. The robust t-statistics are in parentheses. In bold we highlight statistically significant coefficients larger than 0.1; smaller and statistically significant coefficients are in italics.

Figure 4: Asymmetric impact of signed jumps on volatilities of individualcurrencies

Note: For each leading currency, we report on the x-axis the coefficient of the positive signed jumps and on the y-axis the coefficient of negative signed good jumps. Each symbol refers to an exchange rate, and each time zone adopts a different colour.

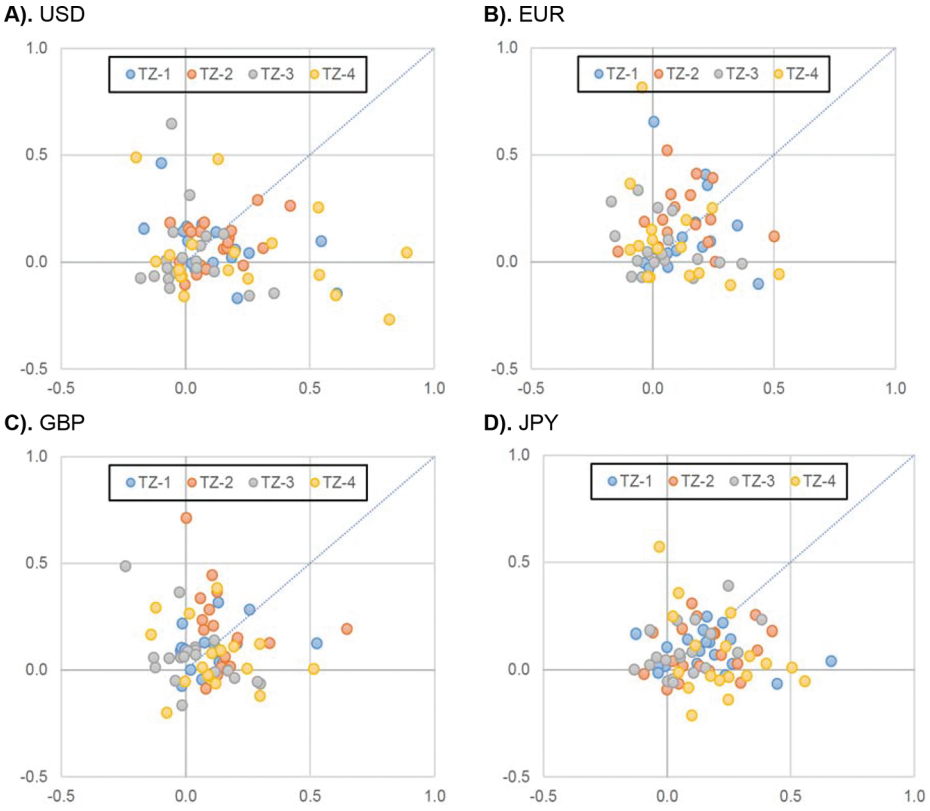

this section, we analyse the asymmetries in the impact of signed volatility over various horizons, by modifying the value of h in Eq. (4). **Figure 5** shows the evolution over time of the coefficients of good and bad volatility for the four time zones and leading currencies. A comparison between RV and its decomposed filtered semivariances is made in **Figure 5**. The point estimates of lagged daily RV come from Eq. (2) and the point estimates of ϕ_d^+ and ϕ_d^- come from Eq. (4), for forecast horizons from 1 to 66 days and with 95% confidence intervals. It is worth noting that Eq. (4) provides

Figure 5: The impact of good and bad volatility over time zones and currency panels

Note: The figure indicates the evolution of the coefficients associated with lagged realized semivariances over increasing levels of *h*. The blue dashed lines refer to the coefficients for good volatility while the continuous red lines refer to the coefficient of bad volatility; finally, dotted lines identify confidence intervals at the 95% level. The grey line refers to the coefficient of the realized variance (for ease of reading, we do not in this case report the confidence interval).

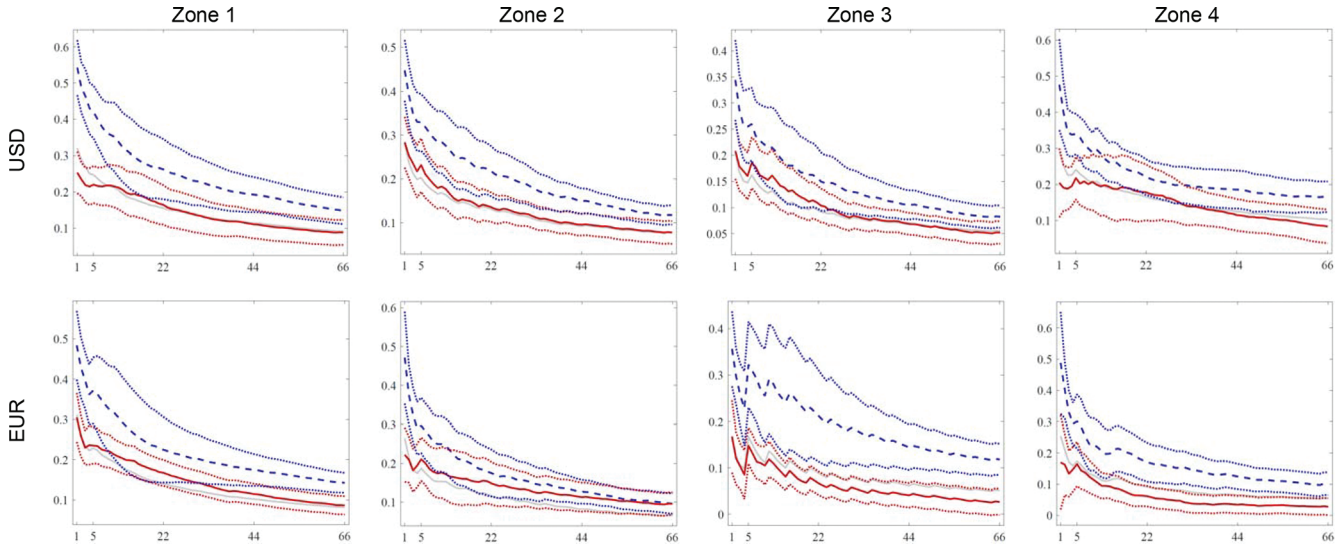

Figure 5: (Continued). The impact of good and bad volatility over time zones and currency panels

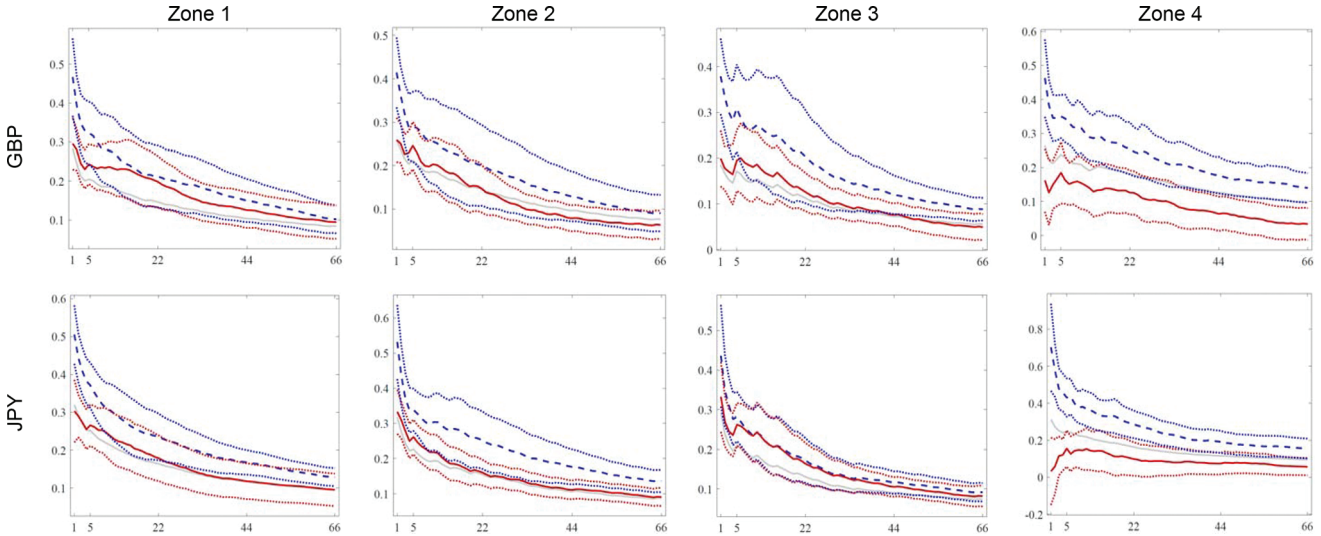

Figure 6: The impact of volatilities over and across time zones

Note: The figure includes the evolution of the coefficients associated with lagged volatility over increasing levels of *h*. The four time zones are presented through four different lines, and dotted lines identify confidence intervals at the 95% level.

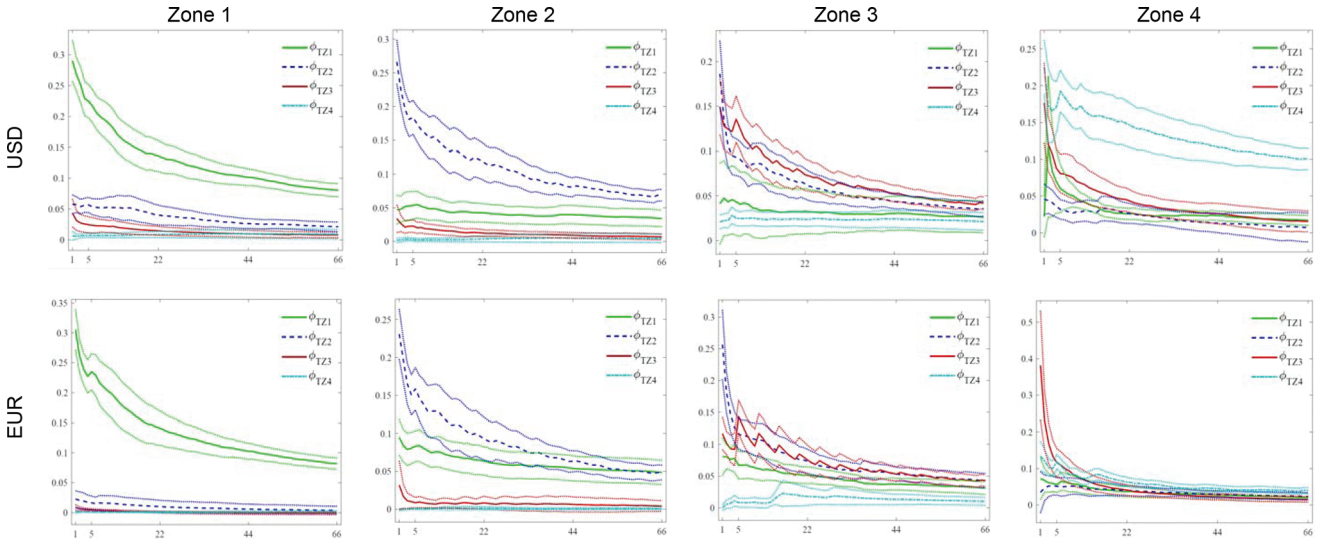

Figure 6: (Continued) The impact of volatilities over and across time zones

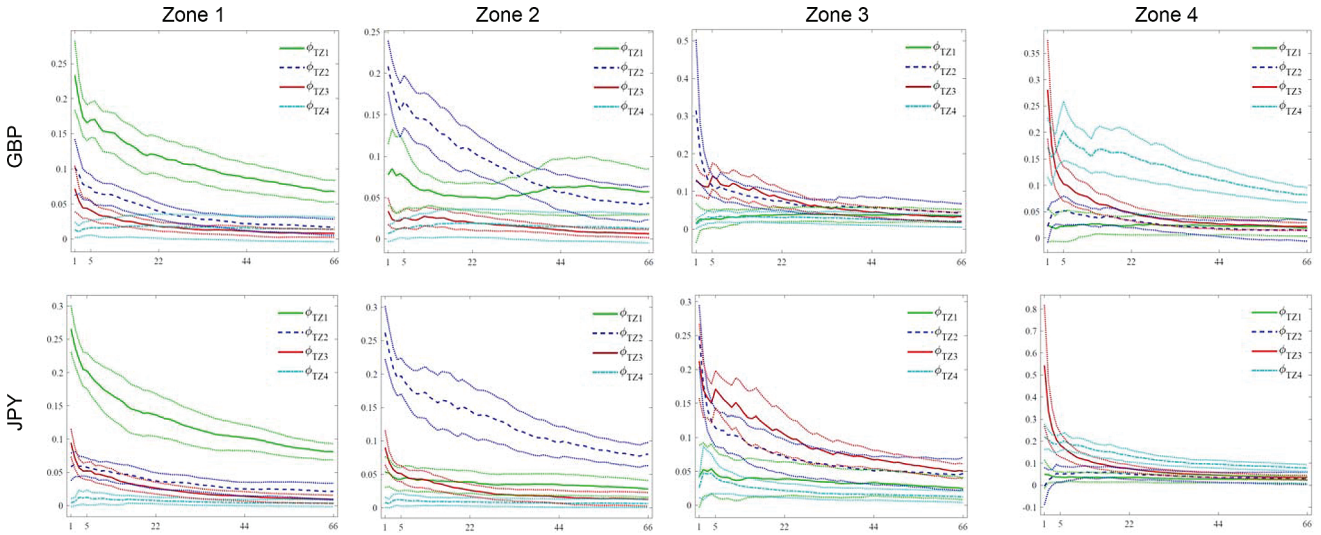

a full decomposition of the RV into filtered signed variations, i.e. positive and negative semivariances after filtering for jumps.

By contrasting the signed volatility effect with the impact associated with the baseline model (the grey line) we note similar patterns in the various sub-plots. Firstly, the models without a decomposition of volatility into good and bad lead to a lagged volatility lying between the values observed for the good and bad cases. The general pattern of how volatility reacts to past good and bad volatility is similar to what we report for the 1-day forecast in Table 3. Secondly, the difference between the influences of semivariances disappear (confidence intervals start to overlap) between 5 and 22 days, and thus the asymmetries between the semivariances is short lived. This confirms that heat waves are diffused in the cross section of exchange rates, coherently with the stylized facts characterizing realized volatility sequences (i.e., strong serial dependence and existence of asymmetric impact from *Good* and *Bad* volatility).

To examine the time horizon effect of meteor showers, we repeat the analysis for all four leading currencies, to forecast the volatilities of the four time zones (with adjustments of appropriate time lags) up to a forecast horizon of 66 days, as in Eq. (3). The point estimates of lagged daily RVs, for four time horizons, for forecast horizons from 1 to 66 days and with 95% confidence intervals are shown in **Figure 6**.

These plots collectively confirm the previous evidence in Table 2 that volatility in time zone 2 impacts volatility in time zone 3 and similarly volatility in time zone 3 impacts volatility in time zone 4. Time zone 1 also has a higher impact on time zone 2 in the case of EUR and GBP. Notably, this meteor shower effect is also significant up to the 22 days ahead volatility forecast. Again, the graphical evidence associated with the horizon effect does not deviate from the interpretation provided for the one-day-ahead forecasts and included in the previous sections. In addition to the previous evidence, beside noticing the long lasting effect due to heat waves, we might also state that this effect appears to be dominating over the meteor showers.

4. Conclusion

In this paper, we examine the local and regional spillover effects among different clusters of four major internationally traded currencies. Using

high-frequency 5-minute exchange rate quotes against the USD, EUR, GBP and JPY from October 1, 2009 to September 30, 2020, we calculate the realized volatilities and jumps for four different time zones. In doing so, we first test for jumps and decompose high frequency FX returns into returns associated with jumps and non-jumps events. Next, we calculate and analyse asymmetries (good versus bad) in continuous (seminavariances) and discontinuous (signed jumps) components of exchange rate evolution. The realized volatilities are highest in case of USD and JPY and lowest in case of EUR. The realized volatility is highest when the trading takes place in Tokyo and Sydney. The positive and negative signed jumps are comparatively higher in the London and NY time zone. The correlation of volatility measures across time zones provide an initial evidence on the regional spillover effects.

Therefore, we examine, through a forecasting exercise, both local (heat wave) and regional (meteor shower) spillover using a basic and an extended panel HAR framework, respectively. The local spillover is found in all pairs of FX and asymmetric effect of positive and negative semivariances on future realized volatility is found only in the short run. Jump variations mostly have a local effect. The regional spillover exists when the trading takes place between London and New York. The information spillover from the US and European trading zone to the US might be due to higher activity by US-based agents. The accumulation of information within a calendar day also affects the following day's exchange rates in the Asian zone. In addition, spillover exits from New York to Tokyo and Sydney. These regional spillover effects are more profound from the bad volatility. Recent surveys of Bank for International Settlement (BIS) show increasing tendency of financial customers (e.g., hedge funds, mutual funds, institutional investors, and other portfolio managers) to participate in foreign exchange trades. This phenomenon is reflection of increasing globalization of forex markets over time, which results in information flows across trading zones. We postulate that existing asymmetries in information flow can be used to formulate viable trading strategies. We have focused on the panel of currencies and hence provide evidence on the aggregate effects, for future studies, it could be interesting to examine the local and regional spillover from major trading currencies to new and emerging European forex markets (see e.g., Kočenda and Moravcová (2019)).

Sign effects of volatility and jumps in forex markets and a reappraisal of meteor showers and heat waves

Internet Appendix

A. Measuring volatility and jumps

Consider a continuous-time stochastic process for log prices, p_t, which consists of a continuous component and a pure jump component:

$$p_t = \int_0^t \mu_s ds + \int_0^t \sigma_s dW_s + J_t, \tag{A.1}$$

where J stands for a pure jump process, μ accounts for the drift of the stochastic process and is locally bounded, and σ is a strictly positive cádlág process. The quadratic variation of this process is:

$$[p,p] = \int_0^t \sigma_s^2 ds + \sum_{0<s\leq t} (\Delta p_s)^2 \tag{A.2}$$

In Eq. (A.2) $\Delta p_s = p_s - p_{s-}$ represents a jump, when one occurs. Andersen et al. (2001) introduce a natural estimator for the quadratic variation of a process as the sum of frequently sampled squared returns, commonly known as realized variance (RV). For simplicity, suppose that prices $p_0,\ldots,p_n$ are observed at $n + 1$ times, equally spaced on $[0,t]$. Using these returns, then-sample realized variance, RV, is defined as below and can be shown to converge in probability to the quadratic variation as the time interval between observations becomes small (Andersen et al., 2003):

$$RV = \sum_{i=1}^{n} r_i^{2p} \underset{\rightarrow}{} [p,p], \quad \text{as } n \to \infty \tag{A.3}$$

where $r_i = p_i - p_{i-1}$

Unlike Patton and Sheppard (2015), we pre-test for jumps through the Lee and Mykland (2008) (LM) test[5] and decompose the series of high

5 Dumitru and Urga (2012) perform a comprehensive Monte Carlo comparison between nine procedures and find that the overall best performance is provided by the Lee and Mykland (2008) approach.

frequency returns into the contribution to the continuous price variance and the contribution to the discontinuous price variance, i.e. the jumps. Since accounting for the periodicity greatly improves the accuracy of intraday jump detection methods, we first apply the Boudt, Croux and Laurent (2011) procedure to filter returns from the intra-day periodicity. This filtering procedure is applied without sub-dividing the data into time zones. Next, we apply the Lee and Mykland (2008) (LM) test for intra-day jump detection. Coherent with LM, we have used a ratio between the intra-day return at time i and the bipower variation based on the data of a particular time zone. Within each time zone, we have different past window size due to difference in number of observations. The window () is based on the formula provided by Lee-Mykland (see page # 2542) i.e., $K = \Delta t^{\alpha}$. Where Δt depends on the no. of observations within each time zone and $-1 < \alpha < -0.5$, we set α=0.49. Furthermore, by referring to the approach we adopt to decompose the volatility into the signed continuous and discontinuous components, we note the following: first, we filter the intra-daily periodicity component without dividing data into time-zones; second, we evaluate the LM test statistic for jump detection at the time zone level, also accounting for the different lengths of the time-zones.

The returns filtered from jumps are used to capture the pure realized semivariances, i.e. realized semivariances not contaminated with the jumps as:

$$RS^{+} = \sum_{i=1}^{n} rc_i^2 I_{[r_i>0]},$$
$$RS^{-} = \sum_{i=1}^{n} rc_i^2 I_{[r_i<0]}. \tag{A.4}$$

where rc are the returns filtered from jumps. On the other hand, for jumps, we compute the discontinuous component of volatility, together with its signed versions. We compute the latter by inferring the sign from the intra-day returns that we "label" as jumps. The three quantities correspond to:

$$\Delta J^2 = \sum_{i \in J} rj_i^2$$
$$\Delta J^{2+} = \sum_{i \in J} rj_i^2 I_{[r_i > 0]} \ ,$$
$$\Delta J^{2-} = \sum_{i \in J} rj_i^2 I_{[r_i < 0]}, \qquad \text{(A.5)}$$

where, rj are the returns associated with jumps and in a given day, J is the set of 5-minute intervals where a jump occurs. Therefore, on the days where no jump component is detected, all the jump measures are exactly equal to 0 and, in a given day, we might have only one signed jump component different from zero. Note that, when measuring the pure realized variance and semivariances for a given day, we evaluate Eq. (A.3) and Eq. (A.4) using the returns set excluding jumps, i.e. all the returns within a day minus the returns included in J.

As we work with time zones, all the quantities (realized volatility, realized semivariances, signed jumps) are evaluated using the data belonging to a specific time zone. For instance, the realized volatility is computed as:

$$RV^{(j)} = \sum_{i \in N_j} r_i^2, \qquad \text{(A.6)}$$

where N_j is the set containing the return time indexes for time zone j. We compute in a similar way both jumps as well as semivariances and signed jumps, starting, in the latter case, from jumps identified at the single time zone level, and excluding jumps from the evaluation of the semivariances.

B. Descriptive analysis

Figure B.1 shows the box plots for the various volatility measures used inthis paper. These boxplots show 5% quantile, 25% quantile, median (or 50% quantile), 75% quantile, and 95% quantile values for realized variance, goodand bad volatility (realized positive and negative semivarinaces) and positiveand negative signed jumps. Average (mean) values are indicated using a plussign. Panels A-D correspond to each leading currency, and within each boxplot,we compare the values for the four selected time

Figure B.1 Boxplots of volatility estimators

Note: These boxplots show the volatility estimates on y-axis for the four time zones mentioned on x-axis. Each boxplot shows 5% quantile, 25% quantile, median (or 50% quantile), 75% quantile, and 95% quantile values of the volatility measures. Average values are shown by a plus sign. The values are scaled by 100.

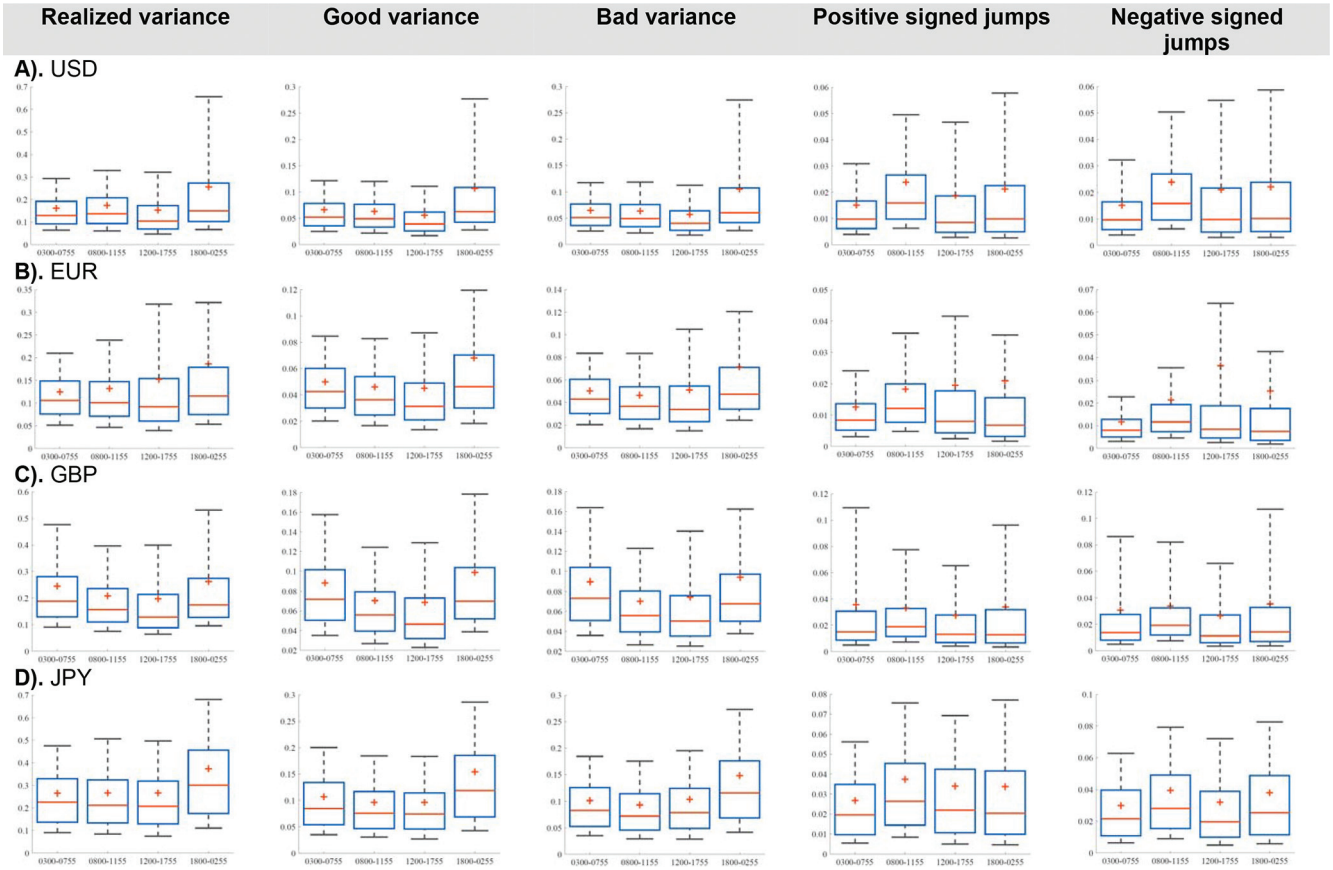

zones. The realizedvolatilities are highest in case of USD and JPY and lowest in case of EUR.Collectively, these boxplots show a few differences across leading currenciesand time zones. For example, the median RV for all four major currencies ishighest in the fourth time zone, which corresponds to trading in Tokyo andSydney. The magnitude of difference among RVs across the four time zones ishighest in the case of USD, while the differences are comparable for EUR andJPY. For GBP, the median RV is also higher in the first time zone,corresponding to trading in London. A similar pattern is observed for positiveand negative semivariances, which are higher in time zone 4. The median valuesof positive and negative signed jumps are comparatively higher in the secondtime zone, London and NY jointly. There are no significant differences betweengood and bad volatilities and jumps within a major currency pair, but they aredifferent across the four time zones.

Figure B.2a shows, in the form of heatmaps, the median values of individual currency correlations among the computed volatility measures. We mediate across the available currencies with respect to a specific leading currency. For all currencies and time zones, the correlation between RS^{+} and RS^{-} ranges between 63% (Pound in time zone 2) and 93% (Pound in time zone 3). The correlation between positive and negative signed jumps ranges from 18% (Euro in time zone 1) to 45% (Euro in time zone 4). The values of the correlation between continuous parts and signed jump parts are considerably lower. These findings indicate that the decomposition of volatility into its continuous and jump components yields interesting information. The correlation between RS^{+} and RS^{-} is generally higher in the fourth time zone, suggesting that good and bad volatilities might occur with similar magnitude. Overall, there are marked differences between the correlations over the four time zones.

The heatmaps in **Figure B.2b** show the median values of individual correlations among RVs across the four time zones. These images show the strength of association of volatilities in the four time zones. The correlation between RVs of time zones 1 and 2 is almost always higher than the correlation among RVs for the other time zone pairs. Relatively, the lowest correlation is evident between the RVs of time zones 3 and 4. Note that the existence of correlation among time zones is evidence of the presence of dynamic interdependence between zones. These correlations are, in effect, equivalent to cross-correlations, highlighting the occurrence

Figure B.2a: Heatmaps of median values of individual correlations among volatility measures

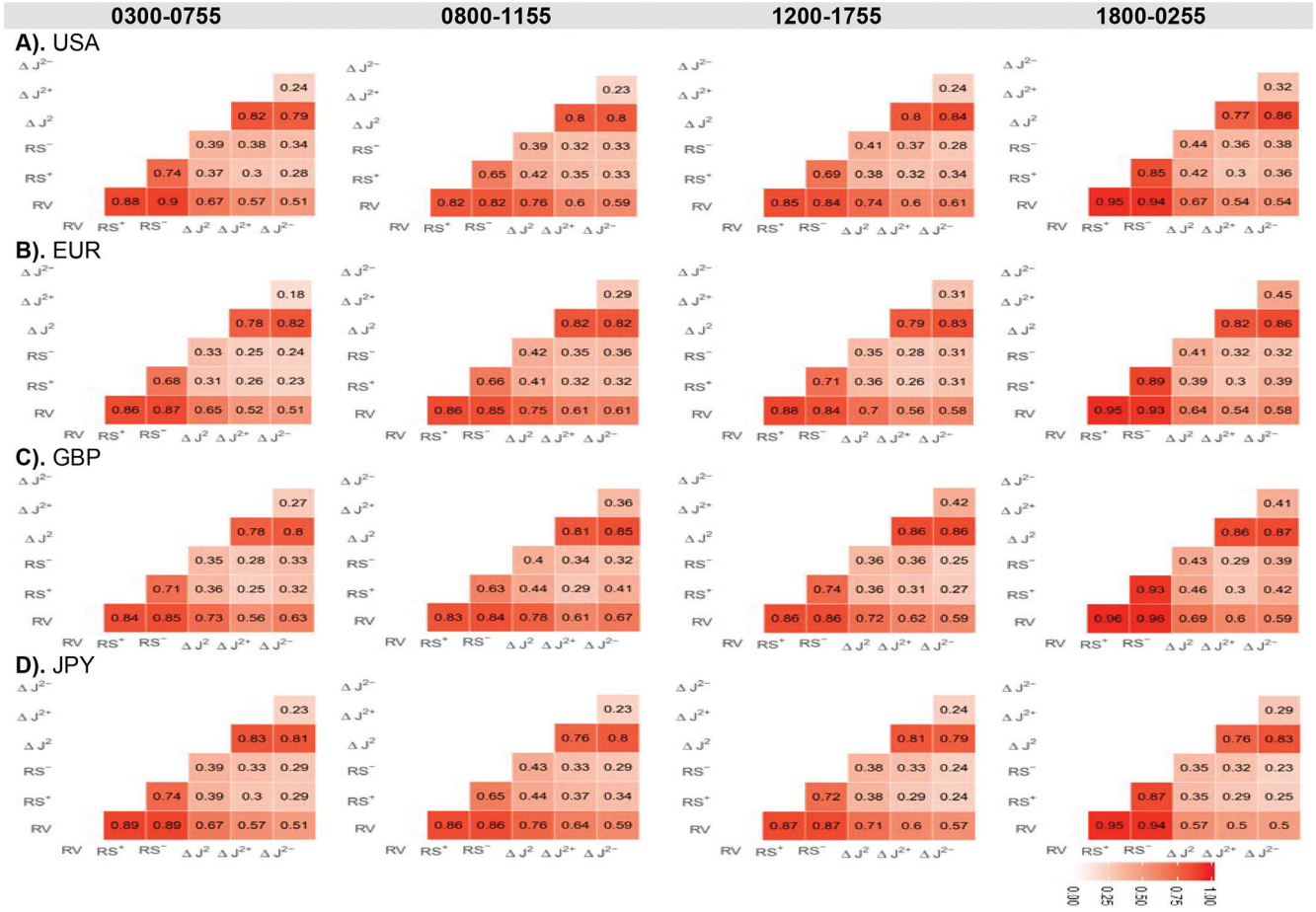

Figure B.2b: Heatmaps of median values of correlations among realized volatilities across time zones

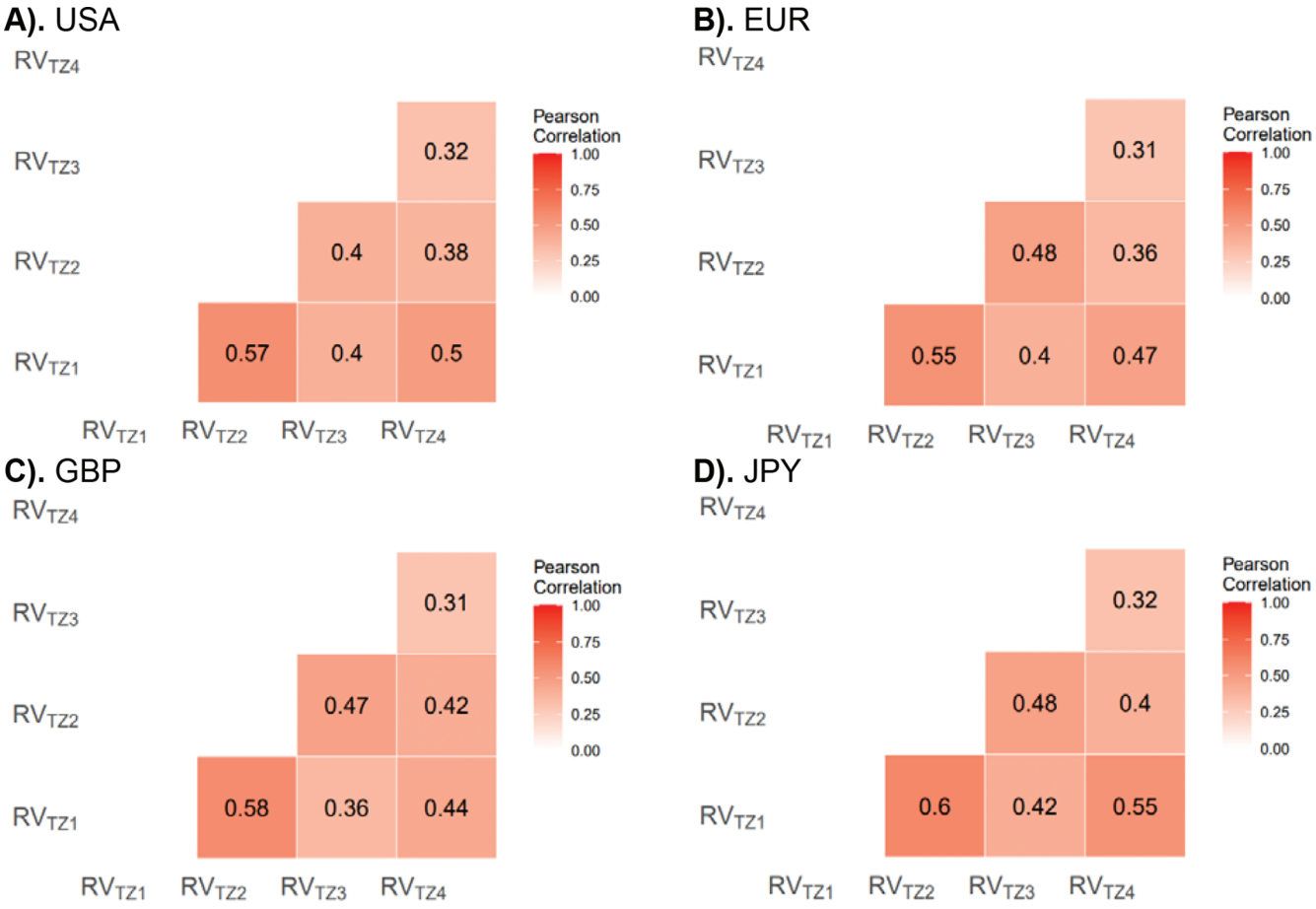

of lead-lag links. This is a consequence of observing the realized quantities over non-overlapping time periods.

C. Model estimation

For parameter estimation we use a weighted least squares (WLS) approach, as in Patton and Sheppard (2015). In doing so, the model is first estimated using ordinary least squares (OLS) and the WLS weights are then constructed as the inverse of the fitted value from that OLS estimation.[6] To recover standard errors we use a Newey and West (1987) heteroskedasticity and autocorrelation consistent (HAC) estimator. We calibrate the Newey-West bandwidth by using the h days lead of the left side variables, thus setting the bandwidth at $2(h - 1)$.

Although individual exchange rate volatility models can be estimated, our primary objective is to obtain the significance of the average effect and therefore we implement and estimate a panel HAR with fixed effects. The panel HAR, in its simplest specification, is given by:

$$\bar{y}_{h,i,t+h} = \mu_i + \phi_d y_{i,t} + \phi_w \bar{y}_{w,i,t} + \phi_m \bar{y}_{m,i,t} + {}_{i,t+h}$$
$$i = 1, \ldots, n_t, \quad t = 1, \ldots, T, \tag{C.1}$$

where the fixed effect μ_i allows each exchange rate to have different levels of long-run volatility. Note that we adopt the specification of Eq. (C.1) for illustrative purposes; in the following sections we generalize the model by the addition of further explanatory indicators as well as by introducing interdependence. Nevertheless, despite the generalized model structure, the estimation approach is the same across all specifications. Let $Y_{i,t} = [y_{i,t}, \bar{y}_{w,i,t}, \bar{y}_{m,i,t}]'$; then the model for the realized variance of each exchange rate can be compactly expressed as:

$$\bar{y}_{h,i,\,t+h} = \mu i + \phi' Y_{i,t} + \epsilon_{i,t+h} \quad i = 1, \ldots, n_t, \quad t = 1, \ldots, T. \tag{C.2}$$

6 Using volatility measures as dependent variables unfortunately results in OLS estimates primarily focusing on the fitting periods of high variance, placing little weight on more tranquil periods. The level of volatility changes significantly over the sample period and the positive relationship between volatility itself and volatility of errors is an important drawback. The WLS is therefore used to capture the heteroskedasticity of model residuals and back it to the level of the process, in line with the standard asymptotic theory for realized measures (Andersen et al., 2003). As an alternative approach, one may use OLS on log volatility. However, such a model predicts log volatility rather than levels of volatility, whereas the latter is the main interest in economic applications.

Now, define $\tilde{y}_{h,i,t+h} = \bar{y}_{h,i,t+h} - \hat{\upsilon}_{h,i}$ and $\tilde{Y}_{i,t} = Y_{i,t} - \hat{\Upsilon}_i$, where $\hat{\upsilon}_{h,i}$ and $\hat{\Upsilon}$ are the WLS estimates of the mean of $\bar{y}_{h,i}$ and Y_i, respectively. Next, the pooled parameters are estimated by:

$$\hat{\phi} = \left(T^{-1} \sum_{t=1}^{T} \left(n_t^{-1} \sum_{i=1}^{n_t} w_{i,t} \tilde{Y} i, t \tilde{Y}'_{i,t} \right) \right)^{-1} \times \left(T^{-1} \sum_{t=1}^{T} \left(n_t^{-1} \sum_{i=1}^{n_t} w_{i,t} \tilde{Y}_{i,t} \tilde{y}_{h,i,t+h} \right) \right), \qquad (C.3)$$

where $W_{i,t}$ are the weights and n_t are the number of firms in the cross section at date t. The asymptotic distribution is used for inference as:

$$\sqrt{T}\left(\hat{\phi} - \phi_0\right) \xrightarrow{d} N\left(\mathbf{0},\ \mathbf{\Sigma^{-1}\Omega\Sigma^{-1}}\right) \quad as\ T \to \infty, \qquad (C.4)$$

where

$\Sigma = \text{plim}_{T\to\infty} T^{-1} \sum_{t=1}^{T} \left(n_t^{-1} \sum_{i=1}^{n_t} w_{i,t} \tilde{Y}_{i,t} \tilde{Y}'_{i,t} \right)$, $\Omega = \text{avar}\left(T^{-1/2} \sum_{t=1}^{T} \boldsymbol{z}_{t+h} \right)$,

and $\mathbf{z}_{t+h} = n_t^{-1} \sum_{i=1}^{n_t} w_{i,t} \tilde{Y}_{i,t} \epsilon_{i,t+h}$.

Comparing our model to the closely related work of Lahaye and Neely (2020) it emerges that our specification might be considered a special case of their proposal. In fact, in Eq. (C.1) we account only for the serial dependence, while the introduction of cross-trading times interdependence is discussed in a following subsection. A further distinctive feature of our approach is that we resort to a panel estimator, thus focusing on the overall behaviour over a panel of currencies, all linked by a common denominator (a leading reference currency). While this seems to be a limited and simplified approach, it allows us to analyse the serial dependence and later the cross-dependence with a large number of exchange rates, without an explosion in the number of covariates as would happen if strictly following Lahaye and Neely (2020), see their Table 2.

D. Extended specifications and additional tables

The following basic and extended specifications are estimated using weighted least squares and Newey and West (1987) HAC to make

Table D.1: The role of continuous and jump components

A. Estimation results for the USD

	ϕ_C^{TZ1}	ϕ_C^{TZ2}	ϕ_C^{TZ3}	ϕ_C^{TZ4}	ϕ_J^{TZ1}	ϕ_J^{TZ2}	ϕ_J^{TZ3}	ϕ_J^{TZ4}	*Adj.* R^2
TZ=1 (London only)	0.399 (15.90)				0.125 (4.73)				0.212
	0.323 (13.04)	0.088 (6.87)	0.061 (2.91)	0.013 (1.93)	0.101 (3.89)	0.023 (1.86)	0.018 (1.54)	−0.010 (−3.41)	0.262
TZ=2 (London and NY)		0.366 (16.74)				0.139 (5.32)			0.203
	0.078 (3.75)	0.310 (13.32)	0.037 (2.24)	0.004 (1.38)	0.012 (1.14)	0.126 (4.83)	0.029 (1.61)	−0.003 (−1.25)	0.231
TZ=3 (NY only)			0.275 (10.53)				0.076 (3.48)		0.101
	0.059 (2.51)	0.047 (2.61)	0.226 (8.71)	0.025 (3.23)	−0.007 (−0.39)	0.016 (0.78)	0.080 (3.70)	−0.005 (−0.46)	0.208
TZ=4 (Tokyo and Sydney)				0.342 (12.59)				0.135 (4.89)	0.436
	0.071 (2.00)	0.042 (2.73)	**0.168** (3.17)	**0.248** (9.84)	−0.024 (−2.17	0.040 (1.88)	**0.187** (4.12)	**0.125** (4.67)	0.479

B. Estimation results for the EUR

	ϕ_C^{TZ1}	ϕ_C^{TZ2}	ϕ_C^{TZ3}	ϕ_C^{TZ4}	ϕ_J^{TZ1}	ϕ_J^{TZ2}	ϕ_J^{TZ3}	ϕ_J^{TZ4}	*Adj.* R^2
TZ=1 (London only)	0.394 (15.96)				0.102 (5.21)				0.17
	0.304 (10.19)	**0.140** (3.40)	0.071 (3.92)	0.000 (0.09)	0.060 (2.75)	0.003 (1.80)	0.001 (0.85)	0.001 (1.92)	0.19
TZ=2 (London and NY)		0.346 (14.33)				0.126 (5.70)			0.07
	0.139 (5.70)	**0.261** (10.99)	0.041 (2.83)	0.000 (0.25)	0.016 (0.95)	0.101 (4.78)	0.030 (1.29)	−0.003 (−1.68)	0.07
TZ=3 (NY only)			0.254 (10.92)				0.041 (1.76)		0.05
	0.077 (5.45)	**0.093** (4.89)	**0.196** (9.03)	0.008 (1.30)	0.007 (0.61)	0.008 (0.55)	0.040 (1.70)	−0.009 (−2.17)	0.13
TZ=4 (Tokyo and Sydney)				0.329 (11.35)				0.058 (2.37)	0.03
	0.128 (2.42)	−0.064 (−1.20)	**0.575** (3.35)	**0.138** (3.67)	0.004 (0.23)	0.086 (1.52)	**0.175** (2.40)	0.047 (1.86)	0.04

Table D.1 (Continued)**:** The role of continuous and jump components

	ϕ_C^{TZ1}	ϕ_C^{TZ2}	ϕ_C^{TZ3}	ϕ_C^{TZ4}	ϕ_J^{TZ1}	ϕ_J^{TZ2}	ϕ_J^{TZ3}	ϕ_J^{TZ4}	*Adj.* R^2
C. Estimation results for the GBP									
TZ=1 (London only)	0.382 (11.69)				0.118 (5.06)				0.344
	0.272 (6.92)	**0.140** (3.05)	**0.118** (3.04)	0.012 (1.00)	0.095 (4.11)	0.029 (1.04)	0.016 (1.21)	0.006 (0.57)	0.357
TZ=2 (London and NY)		0.338 (14.09)				0.150 (6.11)			0.220
	0.107 (3.16)	**0.251** (10.41)	0.073 (3.43)	−0.005 (−0.62)	0.054 (2.21)	0.123 (5.06)	−0.007 (−1.39)	0.016 (1.01)	0.226
TZ=3 (NY only)			0.287 (10.11)				0.044 (2.99)		0.120
	0.035 (1.66)	**0.119** (4.45)	**0.228** (8.21)	0.013 (0.99)	0.024 (1.45)	0.031 (1.19)	0.037 (2.57)	0.024 (1.92)	0.376
TZ=4 (Tokyo and Sydney)				0.314 (12.53)				0.152 (4.64)	0.290
	0.012 (0.45)	0.000 (0.01)	**0.423** (3.74)	**0.188** (6.48)	0.036 (2.41)	0.000 (0.01)	**0.157** (3.18)	**0.150** (5.05)	0.362
D. Estimation results for the JPY									
	ϕ_C^{TZ1}	ϕ_C^{TZ2}	ϕ_C^{TZ3}	ϕ_C^{TZ4}	ϕ_J^{TZ1}	ϕ_J^{TZ2}	ϕ_J^{TZ3}	ϕ_J^{TZ4}	*Adj.* R^2
TZ=1 (London only)	0.407 (12.54)				0.110 (5.78)				0.23
	0.298 (9.40)	**0.089** (4.80)	**0.135** (7.84)	0.002 (0.60)	0.087 (4.69)	−0.001 (−0.08)	0.037 (2.73)	−0.001 (−0.10)	0.28
TZ=2 (London and NY)		0.433 (14.20)				0.106 (4.31)			0.40
	0.114 (3.84)	**0.323** (11.13)	**0.120** (5.18)	0.005 (1.03)	−0.007 (−0.66)	0.057 (2.45)	0.052 (3.10)	−0.002 (−0.25)	0.42
TZ=3 (NY only)			0.383 (7.86)				0.897 (4.17)		0.30
	0.767 (2.88)	**0.783** (2.35)	**0.312** (7.18)	**0.313** (2.82)	0.372 (0.36)	−0.224 (−1.38)	0.922 (4.27)	0.137 (0.97)	0.38
TZ=4 (Tokyo and Sydney)				0.379 (1.88)				0.145 (4.87)	0.29
	0.129 (1.25)	−0.434 (−0.61)	**0.869** (2.92)	**0.127** (2.15)	−0.313 (−1.65)	−0.793 (−1.13)	**0.142** (3.74)	**0.123** (4.99)	0.37

Note: The model is an extended version of the basic HAR model where realized variance is decomposed into its continuous (filtered from jumps) and jump components. These summary results (skipped model co-efficient for lagged weekly and monthly RVs) are for the forecast horizon of one day. In all cases, average values of adj. R^2 for individual currencies are reported. The robust t-statistics are in parentheses.

Table D.2: Direct and indirect convention based on currency shocks

A. USD as the leading currency						
S. No.	**Symbol**	**Country and Currency**	**TZ1**	**TZ2**	**TZ3**	**TZ4**
22.	AUD	Australia Dollar	Indirect	Indirect	Indirect	Indirect
23.	CAD	Canada Dollar	Indirect	Indirect	Indirect	Indirect
24.	CHF	Switzerland Franc	Indirect	Indirect	**Direct**	**Direct**
25.	CZK	Czech Republic Koruna	Indirect	Indirect	**Direct**	Indirect
26.	DKK	Denmark Krone	**Direct**	Indirect	**Direct**	Indirect
27.	EUR	Euro Member Countries	**Direct**	**Direct**	**Direct**	Indirect
28.	GBP	British Pound	**Direct**	Indirect	Indirect	Indirect
29.	HUF	Hungary Forint	Indirect	Indirect	Indirect	Indirect
30.	ILS	Israel Shekel	**Direct**	Indirect	**Direct**	**Direct**
31.	JPY	Japan Yen	Indirect	**Direct**	**Direct**	**Direct**
32.	KRW	South Korea Won	Indirect	Indirect	**Direct**	**Direct**
33.	MXN	Mexico Peso	Indirect	Indirect	Indirect	**Direct**
34.	MYR	Malaysian Ringgit	**Direct**	Indirect	**Direct**	Indirect
35.	NOK	Norway Kroner	Indirect	Indirect	Indirect	Indirect
36.	NZD	New Zealand Dollar	Indirect	Indirect	**Direct**	Indirect
37.	PLN	Poland Zloty	Indirect	Indirect	**Direct**	Indirect
38.	RUB	Russia Rouble	Indirect	Indirect	Indirect	Indirect
39.	SEK	Sweden Krona	Indirect	**Direct**	Indirect	Indirect
40.	TRY	Turkish New Lira	Indirect	Indirect	Indirect	Indirect
B. EUR as the leading currency						
S. No.	**Symbol**	**Country and Currency**	**TZ1**	**TZ2**	**TZ3**	**TZ4**
1.	AUD	Australia Dollar	Indirect	Indirect	Indirect	Indirect
2.	CAD	Canada Dollar	Indirect	Indirect	Indirect	**Direct**
3.	CHF	Switzerland Franc	**Direct**	Indirect	Indirect	**Direct**
4.	CZK	Czech Republic Koruna	Indirect	**Direct**	**Direct**	**Direct**
5.	DKK	Denmark Krone	Indirect	Indirect	Indirect	Indirect
6.	GBP	British Pound	**Direct**	Indirect	Indirect	Indirect
7.	HUF	Hungary Forint	Indirect	Indirect	Indirect	Indirect
8.	ILS	Israel Shekel	Indirect	Indirect	Indirect	**Direct**
9.	INR	India Rupee	**Direct**	**Direct**	Indirect	**Direct**

Table D.2 (Continued)**:** Direct and indirect convention based on currency shocks

10.	JPY	Japan Yen	Indirect	Indirect	Indirect	**Direct**
11.	MXN	Mexico Peso	Indirect	Indirect	Indirect	**Direct**
12.	NOK	Norway Kroner	Indirect	Indirect	**Direct**	Indirect
13.	NZD	New Zealand Dollar	Indirect	Indirect	Indirect	Indirect
14.	PLN	Poland Zloty	Indirect	Indirect	Indirect	Indirect
15.	SEK	Sweden Krona	Indirect	Indirect	Indirect	**Direct**
16.	TRY	Turkish New Lira	Indirect	Indirect	Indirect	Indirect
17.	USD	USA Dollar	Indirect	Indirect	Indirect	**Direct**
C. GBP as the leading currency						
S. No.	**Symbol**	**Country and Currency**	**TZ1**	**TZ2**	**TZ3**	**TZ4**
1.	AUD	Australia Dollar	Indirect	Indirect	Indirect	Indirect
2.	CAD	Canada Dollar	Indirect	**Direct**	Indirect	**Direct**
3.	CHF	Switzerland Franc	Indirect	**Direct**	**Direct**	**Direct**
4.	CZK	Czech Republic Koruna	Indirect	**Direct**	Indirect	**Direct**
5.	DKK	Denmark Krone	**Direct**	Indirect	**Direct**	**Direct**
6.	EUR	Euro Member Countries	Indirect	**Direct**	**Direct**	**Direct**
7.	HUF	Hungary Forint	Indirect	Indirect	Indirect	Indirect
8.	ILS	Israel Shekel	Indirect	**Direct**	**Direct**	Indirect
9.	INR	India Rupee	**Direct**	**Direct**	Indirect	Indirect
10.	JPY	Japan Yen	Indirect	**Direct**	**Direct**	**Direct**
11.	MXN	Mexico Peso	Indirect	Indirect	Indirect	Indirect
12.	MYR	Malaysian Ringgit	**Direct**	**Direct**	**Direct**	**Direct**
13.	NOK	Norway Kroner	Indirect	**Direct**	Indirect	Indirect
14.	NZD	New Zealand Dollar	Indirect	Indirect	Indirect	Indirect
15.	PLN	Poland Zloty	**Direct**	Indirect	Indirect	**Direct**
16.	RUB	Russia Rouble	Indirect	**Direct**	Indirect	Indirect
17.	SEK	Sweden Krona	Indirect	**Direct**	Indirect	Indirect
18.	TRY	Turkish New Lira	Indirect	Indirect	Indirect	Indirect
19.	USD	USA Dollar	Indirect	**Direct**	**Direct**	**Direct**

Table D.2 (Continued)**:** Direct and indirect convention based on currency shocks

D. JPY as the leading currency						
S. No.	**Symbol**	**Country and Currency**	**TZ1**	**TZ2**	**TZ3**	**TZ4**
1.	AUD	Australia Dollar	Indirect	Indirect	Indirect	Indirect
2.	CAD	Canada Dollar	Indirect	Indirect	Indirect	Indirect
3.	CHF	Switzerland Franc	Indirect	**Direct**	**Direct**	Indirect
4.	CZK	Czech Republic Koruna	**Direct**	**Direct**	**Direct**	Indirect
5.	DKK	Denmark Krone	Indirect	Indirect	Indirect	Indirect
6.	EUR	Euro Member Countries	**Direct**	**Direct**	**Direct**	Indirect
7.	GBP	British Pound	**Direct**	Indirect	Indirect	Indirect
8.	ILS	Israel Shekel	Indirect	Indirect	**Direct**	Indirect
9.	INR	India Rupee	Indirect	Indirect	Indirect	Indirect
10.	KRW	South Korea Won	**Direct**	Indirect	Indirect	**Direct**
11.	MXN	Mexico Peso	Indirect	Indirect	**Direct**	Indirect
12.	MYR	Malaysian Ringgit	Indirect	**Direct**	Indirect	Indirect
13.	NOK	Norway Kroner	Indirect	Indirect	**Direct**	Indirect
14.	NZD	New Zealand Dollar	Indirect	Indirect	Indirect	Indirect
15.	PLN	Poland Zloty	Indirect	Indirect	**Direct**	Indirect
16.	RUB	Russia Rouble	Indirect	Indirect	Indirect	Indirect
17.	SEK	Sweden Krona	**Direct**	Indirect	Indirect	Indirect
18.	TRY	Turkish New Lira	Indirect	**Direct**	**Direct**	Indirect
19.	USD	USA Dollar	**Direct**	Indirect	Indirect	Indirect

inference on estimated parameters. The model uses continuous realized variances (filtered from jumps), and jumps. In all cases, average values of adjusted R^2s for individual currencies are reported. The t-statistics (robust) are in parentheses.

Basic $\overline{RV}_{h,t+h} = \mu + \boldsymbol{\phi_C RVf_t} + \boldsymbol{\phi_J J_t} + \phi_w RV_{w,t} + \phi_m RV_{m,t} + \epsilon_{t+h}$

Extended

$$\overline{RV}_{i,l,h,t+h} = \mu + \sum_{j=1}^{4}\left(\phi_{j,C} RVf_{j,l,t-j\Delta t}\right) + \sum_{j=1}^{4}\left(\phi_{j,J} J_{j,l,t-j\Delta t}\right) + \phi_w \overline{RV}_{i,l,w,t} + \phi_m \overline{RV}_{i,l,m,t} + \epsilon_{i,t+h}$$

References

Andersen, T.G., and Bollerslev, T., 1997, Intraday periodicity and volatility persistence in financial markets, Journal of Empirical Finance, 4 (2-3), 115-158.

Andersen, T. G., Bollerslev, T., Diebold, F. X., and Labys, P., 2003, Modeling and forecasting realized volatility. Econometrica, 71(2), 579-625.

Andersen, T. G., Bollerslev, T., Diebold, F. X., and Labys, P., 2001, The distribution of realized exchange rate volatility. Journal of the American Statistical Association, 96(453), 42-55.

Baillie, R.T., and Bollerslev, T., 1991, Intra-day and inter-market volatility in foreign exchange rates, Review of Economic Studies, 58, 565-585.

Barunik, J., Kocenda, E., and Vacha, L., 2017, Asymmetric volatility connectedness on the forex market, Journal of International Money and Finance, 77, 39-56.

Cai, F., Howorka, E., and Wongswan, J., 2008, Informational linkages across trading regions: evidence from foreign exchange markets, Journal of International Money and Finance, 27, 1215-1243.

Corsi, F., 2009, A simple approximate long-memory model of realized volatility. Journal of Financial Econometrics, 7(2), 174-196.

Corsi, F., and Renò, R., 2012, Discrete-time volatility forecasting with persistent leverage effect and the link with continuous-time volatility modeling, Journal of Business and Economic Statistics, 30 (3), 368-380.

Dacorogna, M.M., Muller, U.A., Nagler, R.J., Olsen, R.B., Pictet, O.V., 1993, A geographical model for the daily and weekly seasonal volatility in the FX market, Journal of International Money and Finance, 12 (4), 413-438.

Dumitru, A-M. and Urga, G., 2012, Identifying jumps in financial assets: A comparison between nonparametric jump tests. Journal of Business and Economic Statistics, 30(2), 242-255.

Engle, R.F., Ito, T., and Lin, W.L., 1990, Meteor showers or heat waves? Heteroskedastic intra-daily volatility in the foreign exchange market, Econometrica, 58, 525-542.

Greenwood-Nimmo, M., Nguyen, V.H. and Rafferty, B., 2016, Risk and return spillovers among the G10 currencies. Journal of Financial Markets, 31, 43-62.

Guillaume, D.M., Dacorogna, M.M., Davé, R.R., Muller, U.A., Olsen, R.B., and Pictet, O.V., 1997, From the bird's eye to the microscope: A survey of new stylized facts of the intra-daily foreign exchange markets, Finance and Stochastics, 1, 95-129.

Hilliard, J. E., and Tucker, A. L., 1992, A note on weekday, intraday, and overnight patterns in the interbank foreign exchange and listed currency options markets. Journal of Banking & Finance, 16(6), 1159-1171.

Ito, T., Engle, R.F., and Lin, W.L., 1992, Where does the meteor shower come from? The role of stochastic policy coordination, Journal of International Economics, 32, 221-240.

Kočenda, E., and Moravcová, M. (2019). Exchange rate comovements, hedging and volatility spillovers on new EU forex markets. Journal of International Financial Markets, Institutions and Money, 58, 42-64.

Lahaye, J., and Neely, C., 2020, The role of jumps in volatility spillovers in foregin exchange markets: meteor shower and heat waves revisited, Journal of Business and Economic Statistics, 38 (2), 410-427.

Lee, S. S., and Mykland, P. A., 2008, Jumps in financial markets: A new nonparametric test and jump dynamics. The Review of Financial Studies, 21 (6), 2535-2563.

Melvin, M., and Melvin, B., 2003, The global transmission of volatility in the foreign exchange market. The Review of Economics and Statistics, 85, 670-679.

Muller, U.A., Dacorogna, M.M., Davé, R.D., Olsen, R.B., Pictet, O.V., and von Weizsacher, J.E., 1997, Volatilities of different time resolutions — Analyzing the dynamics of market components, Journal of Empirical Finance, 4 (2-3), 213-239.

Newey, W. K., and West, K. D., 1987, A Simple, Positive Definite, Heteroskedasticity and Autocorrelation Consistent Covariance Matrix, Econometrica, *55*, 703–708.

Ning, C., Dinghai, X., and Wirjanto, T.S., 2015, Is volatility clustering of asset returns asymmetric? Journal of Banking and Finance, 52, 62-76.

Patton, A. J., and Sheppard, K., 2015, Good volatility, bad volatility: Signed jumps and the persistence of volatility. Review of Economics and Statistics, 97(3), 683-697.

Su, F., 2021, Conditional volatility persistence and volatility spillovers in the foreign exchange market. Research in International Business and Finance, 55, 101312.